Environmental and Experimental Botany 226 (2024) 105876

Contents lists available at ScienceDirect

Environmental and Experimental Botany

journal homepage: www.elsevier.com/locate/envexpbot

Research paper

Salt stress alters root meristem definition, vascular differentiation and metabolome in *Sorghum bicolor* (L.) genotypes

Alice Peduzzi [a], Diego Piacentini [a], Elisa Brasili [a,b], Federica Della Rovere [a], Adriano Patriarca [c], Simone D'Angeli [a], Maria Maddalena Altamura [a], Giuseppina Falasca [a,*]

[a] Department of Environmental Biology, Sapienza University of Rome, Italy
[b] NMR-Based Metabolomics Laboratory (NMLab), Sapienza University of Rome, Italy
[c] Department of Chemistry, Sapienza University of Rome, Italy

ARTICLE INFO

Keywords:
Adventitious root anatomy
Phloem
Root metabolome
Salt stress
Sorghum bicolor
Xylem

ABSTRACT

Knowledge on salt tolerance requires further investigation, particularly in plants of agro-food interest. Sorghum is a potentially useful plant because it is a emerging food species that combines high levels of salt tolerance with interesting nutritional characteristics. In sorghum different genotypes respond differently to saline stress and the early events characterizing the salt stress tolerance are not yet fully understood. Moreover, the number of salt resistant genotypes needs to be extended. The genotypes Bianca and Tonkawa are two possible candidates for extending sorghum cultivation to soils characterized by high levels of salinity. The root is the first organ that responds to soil conditions, especially during the initial stages of plant developmental. The research aim was to analyse the root system responses to salt stress (NaCl) of Bianca and Tonkawa genotypes to identify the morpho-functional and metabolic changes that occur during the initial stages of the root system development and to use them as discriminating parameters for assessing the different plant's susceptibility to the salt. The results showed that salt stress negatively affected many morphological and cyto-histological root parameters, from seed germination to root system establishment. The salt altered the root meristem organization and quiescent centre (QC) definition, but similarly in both genotypes. By contrast, it reduced primary root (PR) length and induced a more extended oxidative stress in the adventitious roots (ARs) and lateral root primordia (LRPs) of Tonkawa in comparison with Bianca. The stele area and the number of protoxylem and phloem elements in the ARs were more reduced in 150 mM NaCl-treated Tonkawa seedlings in comparison with those of Bianca. Moreover, the salt enhanced lignin deposition in protoxylem, early metaxylem and endodermis and changed the root metabolic profiles significantly increasing the levels of leucine, isoleucine, alanine, proline, trigonelline, allantoin and glutamine in Bianca compared to Tonkawa. Altogether, specific morpho-anatomical and metabolic differences between the genotypes were identified as discriminating markers of genotype salt susceptibility.

1. Introduction

Over 800 million hectares of fertile land worldwide are affected by excessive salt concentrations, and half of all crop-land will become so by 2050 (Zhang et al., 2019). Most saline soils are in arid and semi-arid regions, but increasing levels of salt in soils are even affecting some temperate regions. It is known that salt might inhibit the expression of key regulatory genes of the cell cycle (e.g., cyclins and cyclin-dependent kinases), leading to a decreased cell number in the root meristem and an inhibition of root growth, thus negatively affecting the plant's ability to efficiently uptake nutrients and water (Balasubramaniam et al., 2023).

The soil salinization mainly consists of an excessive accumulation of water-soluble salts able to release ions, such as sodium (Na^+), potassium (K^+), chloride (Cl^-), and sulfate (SO_4^{2-}), in the rhizosphere, with the most problems for plants caused by Na^+ and Cl^- (Foronda, 2022). High soil salt levels induce osmotic stress and alter the Na^+/K^+ ratio, causing ionic toxicity, altering the absorption of water/nutrients, and unbalancing the redox cellular state by increases in reactive oxygen species (ROS), with negative consequences on plant metabolism and productivity (de Oliveira et al., 2020; Balasubramaniam et al., 2023). Roots and other plant organs have evolved many mechanisms to alleviate the damage caused by high salinity, ranging from physical defenses,

* Corresponding author.
E-mail address: giuseppina.falasca@uniroma1.it (G. Falasca).

https://doi.org/10.1016/j.envexpbot.2024.105876
Received 12 March 2024; Received in revised form 21 June 2024; Accepted 22 June 2024
Available online 29 June 2024

associated with morpho-functional modifications, to metabolic adjustments (Mansour et al., 2021). For example, metabolites such as flavonoids have been shown to increase plant salt tolerance (Yan et al., 2014; Chandran et al., 2019). In accordance, in *Arabidopsis thaliana* and *Ligustrum vulgare*, increased flavonoid levels are induced by salt and treatments with exogenous flavonoids improve the salt tolerance (Agati et al., 2011; Chan and Lam, 2014).

The root is the first sensor of salt stress, and it is the organ that must undergo the greatest modifications in response to stress to allow plant survival. Numerous studies describe the root anatomical modifications induced by salt, with differences among genotypes even within the same species (Acosta-Motos et al., 2017). Moreover, physiological markers, such as hormone contents and changes in proline levels, and molecular markers, such as the expression of genes conferring salt tolerance, transcription factors and metabolic profile-related genes have been identified in response to salt stress (Gupta and Huang, 2014). Furthermore, it is known that salt activates numerous transport systems to sequester Na^+ in the vacuoles and/or to limit its diffusion towards actively growing tissues, preventing interference with the movement of essential elements (Pantha and Dassanayake, 2020). Thus, the ability of plants to tolerate salt depends also on the possibility of excluding and/or compartmentalizing toxic ions (Krishnamurthy et al., 2007; Huang, 2018).

Sorghum bicolor (L.) Moench is the fifth cereal produced globally, especially in arid and semi-arid regions. This crop is important for cultivation in soils with the greatest salinity risk, given its natural ability to grow under harsh environmental conditions with minimal inputs of water and nutrients (Impa et al., 2019; Ren et al., 2022). Sorghum is one of the oldest cultivated cereals, its caryopses are gluten-free with a high protein and nutrient content and represent a staple food for many poor populations. Moreover, the great efficiency due to its C4 metabolism gives sorghum rapid growth and high yield (Moreno-Villena et al., 2022), especially in soils compromised by salinity and water availability. For these characteristics, sorghum is considered a pioneer crop for marginal lands (Shi et al., 2023). Although salt tolerance is genotype-specific, some sorghum genotypes are tolerant to this stress by activating different resistance mechanisms (Henderson et al., 2020). Even if some individual parameters have been shown to be useful indicators for identifying sorghum genotypes tolerant to salt stress (Huang, 2018), a full identification is still underway. For example, the increase of proline and hydrocyanic acid in roots and leaves of sorghum exposed to salt recovers osmotic balance and antioxidant capacity (Huang, 2018; Calone et al., 2020). Additionally, some membrane transport systems, which help to retain essential ions and exclude or compartmentalize sodium ions, increase in salt tolerant sorghum genotypes, together with a remodeling of membrane lipids, and modifications in cell wall constituents leading to cell wall lignification (Mansour, 2014; Mansour et al., 2020; Karumanchi et al., 2023). In particular, in the roots of a salt-tolerant sorghum genotype thick and lignified cell walls have been shown to occur in the hypodermis and endodermis. The secondary wall thickness and the number of lignified cells in the hypodermis increase with salt stress, and the Casparian strip thickenings of the endodermis show homogenous lignin distribution (Karumanchi et al., 2023). Furthermore, it has also been reported that a salt-sensitive sorghum genotype exposed to salt stress develops a more suberized Casparian strip compared to a sensitive genotype (Abuslima et al., 2022). These results indicate that an apoplastic barrier can form in sorghum roots in response to salt stress and in different ways depending on the genotype.

After a two weeks culture on a synthetic medium, it is known that sorghum seedlings show a root system composed of primary root (PR), nodal roots, which must be considered adventitious roots (ARs) due to their origin, and lateral roots (LRs) (Mohanavel et al., 2020). Despite the vast literature on sorghum responses to salt, there is still a significant lack of information on the morphological, cyto-histological and metabolomic adaptations related to salt susceptibility that occurs in the entire root system and in the ARs, i.e., the main component of the adult plant root system, in particular. Information is mainly lacking on root meristem development and for vascular differentiation.

The potential modifications that salinity can induce in the roots may help to characterize elements useful for defining salt susceptibility, as a prerequisite for the early selection of new salt-tolerant genotypes. For this reason, Tonkawa and Bianca, two grain sorghum genotypes, selected by an italian company leader in the production and marketing of crop seeds, up to now not yet characterized for salt susceptibility/resistance, were chosen for the research. The aim was to analyse the salt stress responses of their root systems to identify morpho-functional and metabolic changes occurring during the initial stages of root system development, which can be used as discriminating parameters for salt susceptibility/tolerance.

The results highlight that the salt negatively affects specific aspects of root anatomy. In fact, when applied at 150 mM, it reduces the PR length and induces a more extended oxidative stress in the roots of Tonkawa in comparison with Bianca. The same salt concentration causes a less sclerification of the pith parenchyma, a reduction of the stele area and of the number of protoxylem and phloem cells in the same genotype in comparison with the other. Moreover, the salt enhances the lignin deposition in the protoxylem, early metaxylem and endodermis of Tonkawa and changes its metabolic profiles lowering the levels of specific metabolites. The relationships between root cyto-histological modifications, metabolomic changes and genotype response are discussed and interpreted as selective markers of salt susceptibility *vs* tolerance.

2. Materials and methods

2.1. Plant materials and growth conditions

Forty-five seeds of Tonkawa and Bianca *Sorghum bicolor* (L.) Moench genotypes (provided by Padana Sementi Elette S.r.l.) were surface sterilized with 70 % (v/v) ethanol for 1.5 min, rinsed 3 times in dH_2O, then soaked in a solution of 40 % (v/v) sodium hypochlorite (15 % Cl active chlorine) on an orbital shaker at 300 rpm for 25 min and then rinsed 4 times in sterile dH_2O (Ronzan et al., 2018). Afterwards, the seeds were sown in sterile poly-ethylene terephthalate (PETG) vessels with a rectangular base (11.4× 8.6× 10.2 cm) (Phytatray™ II, Sigma-Aldrich, Saint Louis, MO, USA), each containing 100 mL of half-strength ($2.1 gL^{-1}$) Murashige and Skoog (MS) salt medium (Murashige and Skoog, 1962), 1 % sucrose and 0.8 % agar, adjusted to pH 5.6–5.8 (Control medium). Salt treatments were performed by adding 50, 100, 150 or 300 mM NaCl to the Control medium. Salt concentrations were selected in accordance with literature data (El Omari and Nhiri, 2015; Dehnavi et al., 2020), even if, the concentration of 300 mM NaCl, sub-lethal for other sorghum genotypes (Mbinda and Kimtai, 2019) was also used. Each culture medium was sterilized at 120°C for 20 min in an autoclave. Sowing was carried out under sterile conditions using a laminar flow hood. Fifteen seeds per treatment, distributed in 5 Phytatrays (3 seeds per phytatray), were kept in a growth chamber with a long-day regime (16 h light/8 h dark) for 10 days at 150 μE $m^{-2}s^{-1}$ intensity of white light and under controlled temperature (25°C light/24°C dark). The relative humidity inside the vessel was about 98–99 %.

Ten seeds for each genotype were also sown in pots filled with bed soil, with no salt addition, and grown, for three months, at the same temperature and photoperiod as in *in vitro* culture.

2.2. Germination percentage and morphological analyses

The germination percentage was evaluated at 24 h, 4, and 10 days on seeds exposed or not to 50, 100, 150 or 300 mM NaCl. On day 10, fifteen plants per genotype and treatment were taken and used for the morphological analyses. Fresh total biomass and fresh root biomass

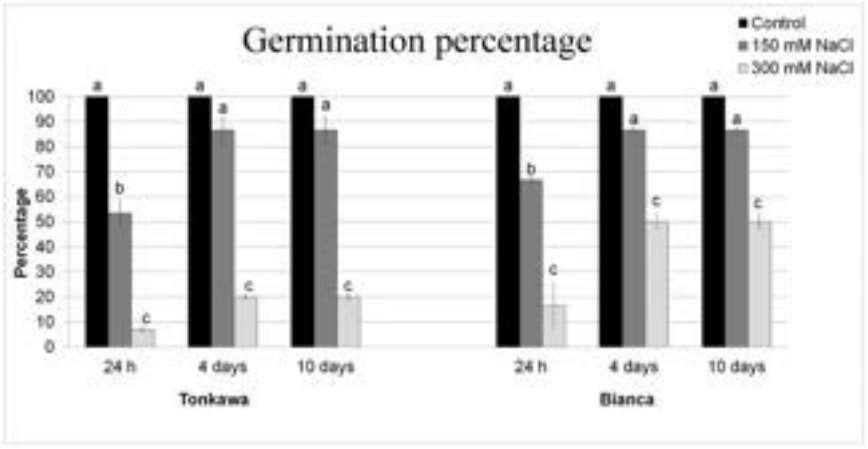

Fig. 1. Mean percentage (±SE) of sorghum Tonkawa and Bianca germinated seeds after 24 h, 4 days and 10 days of exposure to 150 or 300 mM NaCl. Data from three biological replicates. Letters show significant differences for at least $p < 0.05$ within the same data point and genotype. The same letter shows no significant difference within the same data point and genotype. N = 45.

were measured with a sensitivity analytical balance (ATP 220–5DNM, Kern & Sohn, Balingen, Germany). Each plant was photographed with a Canon EOS2000, the corresponding images were processed with ImageJ v1.53c software (Wayne Rasband, National Institutes of Health, Bethesda, USA), and PR and ARs were measured with RootNav v1.8.1 software (Pound et al., 2013).

Based on the morphological results (see Results section), the 50, 100 and 300 mM NaCl treatments were excluded from the subsequent analyses.

2.3. Localization and quantification of superoxide

The intracellular localization and quantification of superoxide anion ($O_2^{\cdot-}$) in Tonkawa and Bianca roots were performed after exposure or not to 150 mM NaCl using the Nitro Blue Tetrazolium (NBT; Roche Diagnostics Corp., GmbH, Germany) assay. The NBT assay relies on a highly specific reaction between NBT and $O_2^{\cdot-}$, producing a purple/blue precipitate called formazan. This precipitate is easily visible in plant cells using a light microscope and it can be quantified using UV-Vis spectrophotometric analysis (Demecsová et al., 2020). For intracellular $O_2^{\cdot-}$ root localization, the first 3 cm from the root tip of PRs and ARs from 3 different 10-day-old plants per genotype, exposed or not to 150 mM NaCl, were incubated in the dark for 30 min with a solution of 0.5 mg mL^{-1} NBT in 10 mM Tris-HCl (pH 7.4) (Piacentini et al., 2020). After having stopped the reaction by transferring the samples into distilled water, they were kept in a chloral hydrate solution [$Cl_3CCH(OH)_2$] and instantly observed with a LEICA DMRB light microscope (Leica Microsystems, Germany) equipped with Nomarski optics.

The quantification of $O_2^{\cdot-}$ was performed following the procedure suggested by Demecsová et al. (2020) with slight modifications. Briefly, approximately 100 mg (fresh weight) of roots per genotype, exposed or not to 150 mM NaCl, were weighed using an analytical balance (Kern ABT 220–5DNM; Kern & Sohn, Balingen, Germany). The samples were incubated in the dark at room temperature for 1 hour and 30 minutes, including 15 minutes under vacuum, in a solution containing 1.2 mM NBT and 10 mM sodium azide (NaN_3; Sigma-Aldrich, Milan, Italy) in 20 mM sodium phosphate buffer (pH 6.0). A root sample incubated only with 10 mM sodium azide (NaN_3; Sigma-Aldrich, Milan, Italy) in 20 mM sodium phosphate buffer was used as blank. After incubation, the roots were rinsed with distilled water and homogenized with a mortar and pestle using liquid nitrogen. The homogenates were then suspended by adding in sequence 360 µL of 2 M potassium hydroxide (KOH; Sigma-Aldrich, Milan, Italy), 440 µL of dimethyl sulfoxide (DMSO; Duchefa Biochem, Haarlem, the Netherlands), and 400 µL of 2-propanol (Carlo Erba, Rome, Italy). The mixture was centrifuged (Micro Star 17 centrifuge, VWR, Milan, Italy) for 5 minutes at 10,000 rpm. After centrifugation, the supernatants were collected, and the $O_2^{\cdot-}$ content was detected by measuring the formazan absorbance at a wavelength of 630 nm using UV-Vis spectrophotometry (Shimadzu UV-1280; Shimadzu, Kyoto, Japan). The absorbance signal recorded at 630 nm for each treatment and genotype was normalized by the weight of each sample (absorbance g^{-1}).

2.4. Cyto-histological analyses

After 10 days from sowing, the apical regions (about 2.0 cm from the root tip) of 3ARs per genotype, exposed or not to 150 mM NaCl, were fixed in 70 % (v/v) ethanol, dehydrated with an ethanol series and embedded in Technovit 7100 (Heraeus Kulzer, Germany). Longitudinal and cross Section (9 µm in thickness) were cut with a HM 355 S microtome (Epredia™, USA), stained with 0.05 % toluidine blue, and observed under a Leica DMRB light microscope (Leica Microsystems, Germany). Images from 9 different cross sections per genotype and treatment, performed in the AR differentiated region, were acquired with a light microscope equipped with an OPTIKA C-P20CC microscope camera (Optika, Italy) and processed with Proview software (version 4.11). The acquired images were measured with ImageJ software (version 1.53c, Wayne Rasband, National Institutes of Health, Bethesda, USA) to evaluate the mean area of the entire root, the stele, the protoxylem, the early metaxylem, the late metaxylem and the phloem elements. The same cross sections were used to detect the mean number of protoxylem, early metaxylem, late metaxylem and phloem elements. To analyse the phloem, the differentiated regions of six ARs per genotype, exposed or not to 150 mM NaCl, were also embedded in agar (4 %w/v). Cross sections of 300 µm in thickness were obtained with a TPI Vibratome Series 1000 sectioning system (TPI, USA) and then stained with 0.005 % aniline blue in 0.07 M phosphate buffer (pH 9.0) (Currier and Strugger, 1956). Afterward, the sections were observed under epifluorescence light with a Leica DMRB microscope equipped with filter "A" (ex. 340–380 nm BP/ Em.425 nm LP), and the images were acquired with an OPTIKA C-P20CC microscope camera. To detect the lignin deposition in the cell walls of the protoxylem, early metaxylem and endodermis, 9 cross sections, from the differentiated region of 3 ARs per genotype exposed or not to 150 mM NaCl, were observed with Leica DMRB light microscope equipped with the same filter as above. The lignin autofluorescence signal was quantified by a multi-point detection and by assigning to each pixel a value ranging from 0 (pure black) to 255 (pure white) of Arbitrary Units (A.Us) by ImageJ software (version 1.53c, Wayne Rasband, National Institutes of Health, Bethesda, USA). To complete the analyses in the late metaxylem elements and the

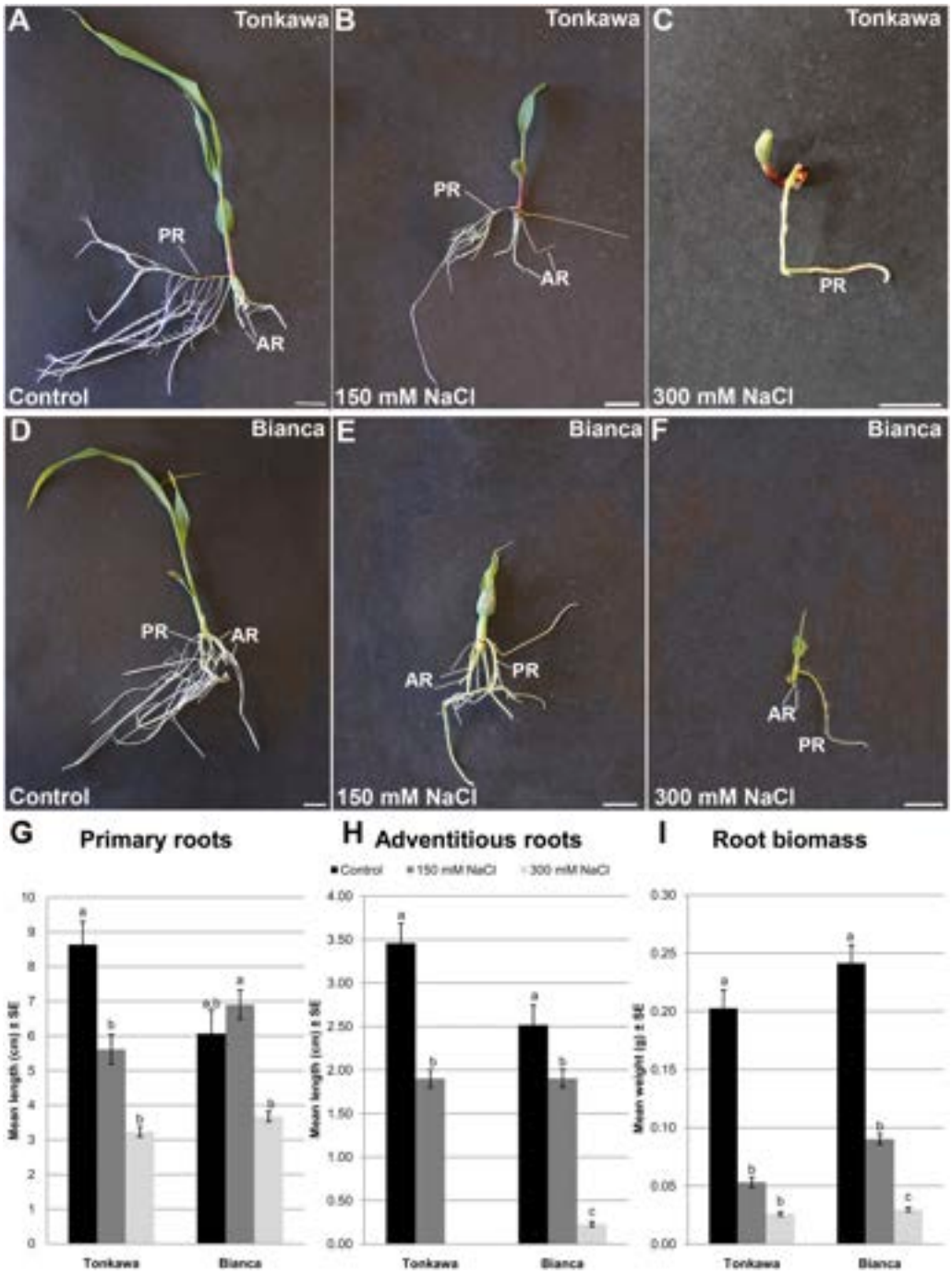

Fig. 2. Tonkawa and Bianca seedlings non-exposed to NaCl (Control; A, D), or exposed to 150 mM (B, E) or 300 mM (C, F) NaCl after 10 days from sowing. Mean length (±SE) of primary roots (G), adventitious roots (H) and mean weight (±SE) of root biomass (I) of Tonkawa and Bianca seedlings non-exposed (Control) and exposed to 150 and 300 mM NaCl. AR: nodal adventitious root; PR: primary root. Bars = 1 cm. Images and data from three biological replicates. Letters show significant differences for at least $p < 0.05$ within the same genotype. The same letter shows no significant difference within the same genotype. N = 45.

differentiated regions of the ARs of both genotypes grown for 1–3 months in pots were also dissected. The sections, obtained by embedding the ARs in agar (4 % w/v) and then sectioning them with a TPI Vibratome Series 1000 sectioning system, were processed to detect the lignin deposition on the cell walls of these elements as reported above.

2.5. Metabolomic analyses

2.5.1. Sample preparation

A total of 0.5 g of fresh roots (coming from 6 pools of 3–4 plants per treatment) was weighed and extracted following a modified Bligh–Dyer protocol (Giampaoli et al., 2021). Briefly, each sample was ground in a mortar with liquid nitrogen and added to a cold mixture composed of chloroform (2 mL), methanol (2 mL), and water (1.3 mL). The samples were stirred, stored at 4 °C overnight and then centrifuged for 30 min at 4 °C with a rotation speed of 11,000 rpm. The upper hydrophilic and the lower organic phases were carefully separated and dried under nitrogen flow. The dried residue of the hydrophilic phase was dissolved in 700 µl D_2O solution of 3-(trimethylsilyl)- propionic-2,2,3,3-d4 acid sodium salt (TSP, 2 mM) as an internal chemical shift and concentration standard. The hydrophilic phase was analyzed by ^{1}H NMR.

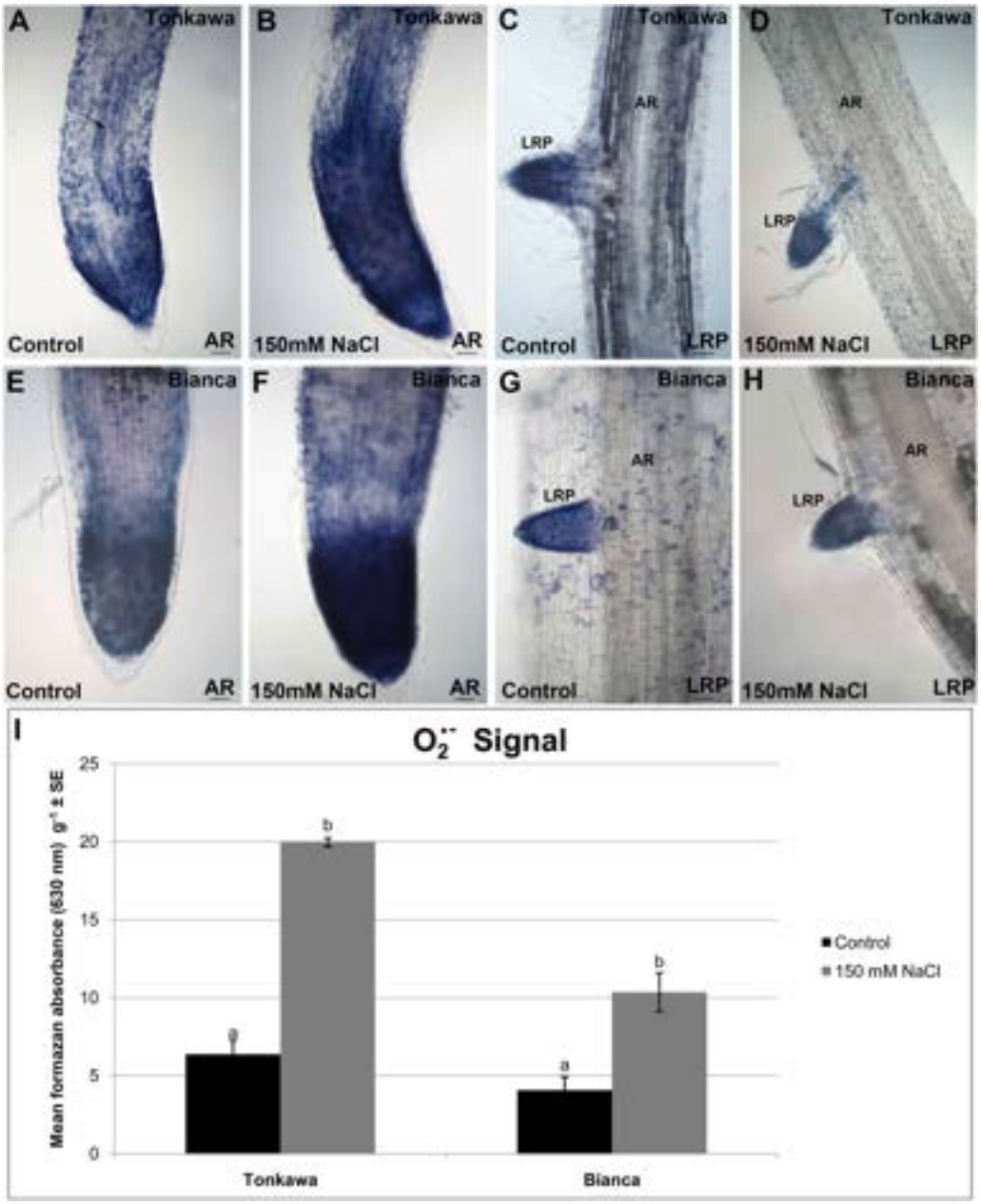

Fig. 3. NBT histochemical analysis (A-H) showing $O_2^{\bullet-}$ staining in the adventitious roots (ARs) and lateral root primordia (LRPs) of Tonkawa and Bianca seedlings grown for 10 days in the absence (A, C, E, G, Control) or in the presence of 150 mM NaCl (B, D, F, H). Images and data from the three biological replicates. The arrow in A shows the differentiating vasculature. Bars = 50 μm. I, mean values (±SE) of formazan absorbance at 630 nm in roots treated or not with 150 mM NaCl. Letters show significant differences for at least $p < 0.05$ within the same genotype. N = 3 independent clusters of root systems per genotype and treatment.

2.5.2. NMR Experiments

The NMR experiments were carried out at 298 K on a JNM-ECZ 600 R (JEOL Ltd., Tokyo, Japan) spectrometer operating at the proton frequency of 600 MHz and equipped with a multinuclear z-gradient inverse probe head. The monodimensional ^{1}H NMR experiments were carried out for quantitative analysis, employing a pre-saturation pulse sequence for water suppression with a time length of 2 s, a spectral width of 9.03 KHz and 64 k data points, corresponding to an acquisition time of 5.81 s. The pulse length of 90° flip angle was set to 8.3 μs, the recycle delay was set to 5.72 s. Monodimensional ^{1}H spectra were analyzed by ^{1}D NMR (DELTA JEOL Ltd., Tokyo, Japan). Bidimensional ^{1}H–^{1}H TOCSY and ^{1}H–^{13}C HSQC experiments were acquired according to Spinelli and co-workers (Spinelli et al., 2022) for the resonance assignment. Quantities were expressed in mg/100 g through comparison of the relative integrals with the reference concentration and normalized to the number of protons (TSP: 9 protons) and to the starting fresh weight of the sample.

2.6. Statistical analyses

All the morphological data and the data of formazan absorbance signal were statistically analysed using a one-way ANOVA test followed by Tukey's post-test (at least at $p < 0.05$) or non-parametrical t-test Kruskal Wallis (Stevens, 2007) after having performed Shapiro–Wilk's normality test. The statistical analyses were carried out through GraphPad Prism 9.3.0 software (GraphPad Software, San Diego, CA, USA). For the analyses of cytohistological data, a two-way ANOVA followed by Tukey's multiple comparisons test (at least at $p < 0.05$) was performed. The above-mentioned experiments were performed in three biological replicates with similar results.

Metabolomic data were statistically analysed using MATLAB®

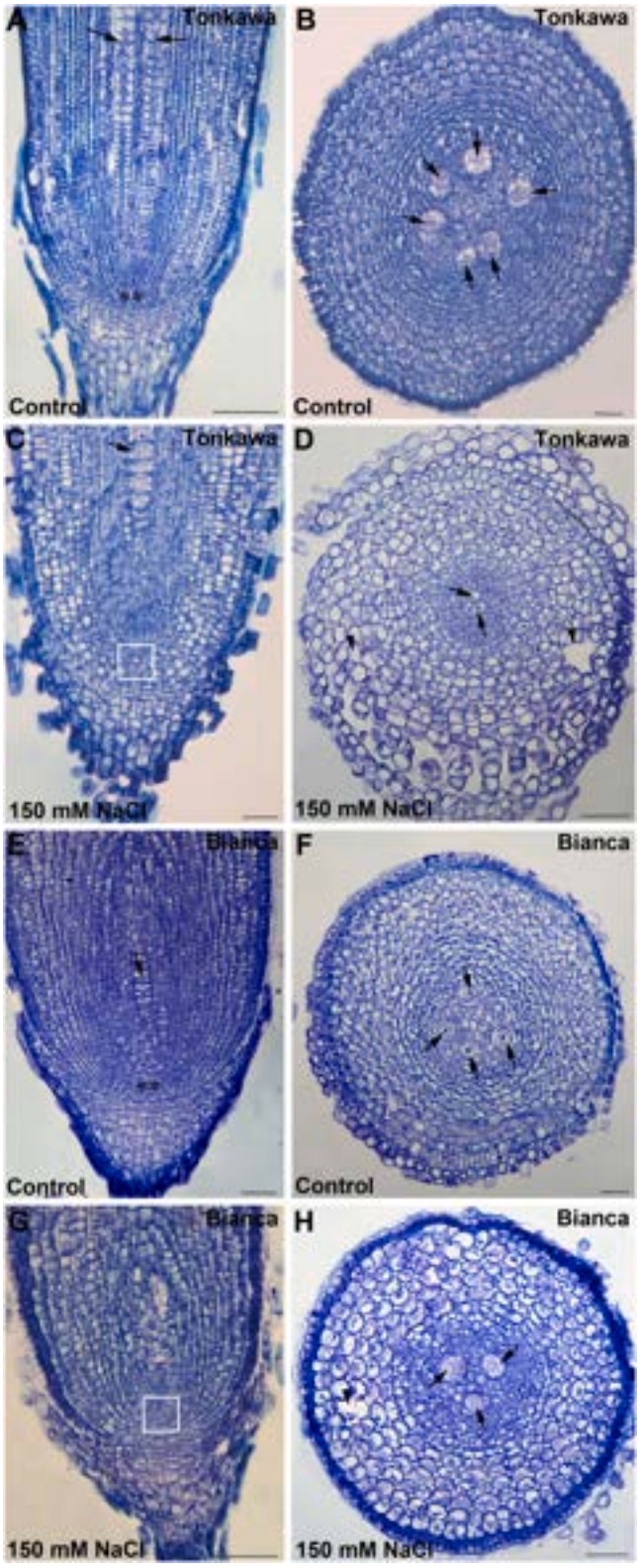

Fig. 4. Longitudinal (A,C,E,G) and transverse (B,D,F,H) sections of Tonkawa and Bianca AR apices non-treated (A,B, E,F, Control) or treated with 150 mM NaCl (C,D, G,H) for 10 days, stained with toluidine blue. Arrows show immature late metaxylem cells. Arrowheads show precocious aerenchyma formation. Asterisks show a correct root quiescent centre. Rectangles show an altered root quiescent centre. Images from the three biological replicates. Bars = 50 μm.

R2023a (MathWorks, Natick, Massachusetts, USA) with the Statistics and Machine Learning Toolbox package used for univariate and multivariate analysis, with a home-built script. Multivariate principal component analysis (PCA) was performed on the data matrix. Data were mean-centered, since the variables with the largest response could dominate the PCA, and then auto-scaled to equalize the importance of the variation of each variable (Eriksson et al., 2013). Error bars of each PCA Loadings were estimated by 1000 bootstrap procedures (Babamoradi et al., 2013). Univariate one-way ANOVA was performed. The Shapiro-Wilk test was performed on each variable to assess data normality prior to one-way ANOVA, while to verify the homoscedasticity condition, the Brown Forsythe test (Brown and Forsythe, 1974) was carried out, with a significance value of 0.05. If these conditions were not met, a non-parametric ANOVA test was carried out with the Kruskal-Wallis test (Stevens, 2007). For the ANOVA-positive variables, with the Bonferroni test (Peluso et al., 2021), the pairwise multiple comparison test was applied to determine which categories were discriminated by the metabolites ($p < 0.05$). Spearman's correlation Heatmap was also done for each harvesting time employing a home-built script.

3. Results

3.1. Salt stress similarly reduces seed germination in the two genotypes, but differently affects root system growth

3.1.1. Germination is reduced by the highest salt concentrations

The germination in the Control plants was 100 % for both Tonkawa and Bianca genotypes already 24 h after sowing (Fig. 1). Similarly, in the presence of 50 mM NaCl the germination after 24 h from sowing was about 100 % in both genotypes (data not shown). The germination trend in the two genotypes exposed to 100 mM NaCl was similar to that observed in the presence of 150 mM. In the presence of the latter concentration there was a delay in the germination with 54 % of germinated seeds in Tonkawa and 67 % in Bianca. At day 4, 87 % of the seeds from both genotypes exposed to 150 mM NaCl had germinated (Fig. 1), and this percentage remained constant until the culture end (day 10). The treatment with 300 mM NaCl strongly inhibited the germination in Tonkawa. In fact, 7 % of the seeds had germinated after 24 h from sowing and only 20 % after 4 days, without any further increase until the culture ended. Differently, Bianca seeds showed greater germination capacity in the presence of 300 mM NaCl, since 17 % and 50 % of the seeds had germinated after 24 h and 4 days, respectively (Fig. 1).

3.1.2. Root system growth is altered by NaCl with differences between the genotypes

To verify the root system response of Tonkawa and Bianca to salt treatments, the PR and AR length, and the root biomass were analysed after the exposure to 50, 100, 150 and 300 mM NaCl. In both genotypes the exposure to 50 mM NaCl did not induce a significant difference in the PR and AR length in comparison with the Control (data not shown). Similarly, the root biomass did not change significantly in Bianca and Tonkawa exposed to 50 mM NaCl (Supplementary Fig. S1). In Tonkawa the PR mean length was similarly and significantly ($p < 0.01$) reduced by both 100 and 150 mM NaCl in comparison with Control and it was even more reduced by 300 mM NaCl (Fig. 2A-C, G). The mean length of ARs was significantly ($p < 0.01$) reduced by 100 and 150 mM NaCl treatments, and completely inhibited by 300 mM (Fig. 2A-C, H). Overall, the root biomass of Tonkawa underwent a significant reduction in the presence of 150 mM NaCl, worsening when exposed to the higher salt concentration (Fig. 2I and Supplementary Fig.1).

Bianca showed a significant ($p < 0.01$) reduction of the PR mean length, in comparison with Control, but only in the presence of 300 mM NaCl (Fig. 2D-F, G). On the contrary, AR mean length was already reduced by 100–150 mM NaCl, and this reduction increased with 300 mM (Fig. 2D-F, H). Also, in Bianca as in Tonkawa, the entire root

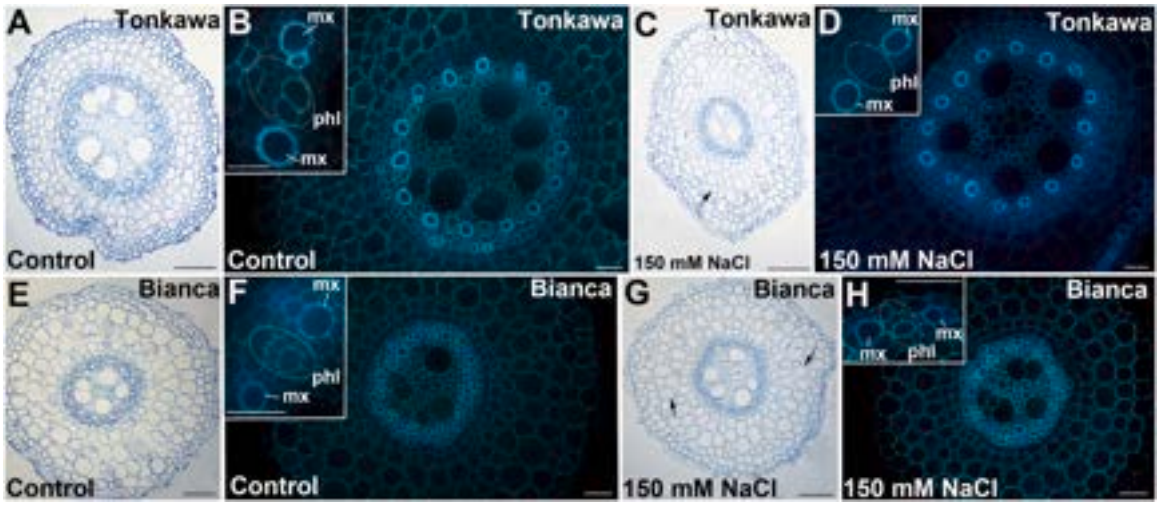

Fig. 5. Transverse sections of the differentiated region of Tonkawa and Bianca ARs, non-treated (A,B,E,F, Control) or treated (C,D,G,H) with 150 mM NaCl for 10 days. A, C, E, G, light microscope images of sections stained with toluidine blue. B, D, F, H, and Insets epifluorescence images of sections stained with aniline blue. Images from the three biological replicates. Ovals in the Insets show the phloem arches. Arrows show plasmolysis in the cortical cells; mx, metaxylem; phl, phloem. Bars = 10 μm (Inset in D); 25 μm (Insets in B, F,H); 50 μm (A-H).

biomass underwent a significant ($p < 0.01$) reduction in the presence of 150 mM of the salt, which was further accentuated at 300 mM (Fig. 2I and Supplementary Fig. 1).

The morphological data of Bianca and Tonkawa root systems exposed to 100 mM NaCl, were similar to those obtained with 150 mM NaCl, and were not reported in the graphs.

Based on the results of germination and root system morphology, the following analyses were

carried out on the two genotypes exposed or not to 150 mM NaCl.

3.2. Salt induces oxidative stress in the roots of both genotypes, but mainly in Tonkawa

The presence of $O_2^{\bullet-}$ in ARs and LRPs, and its variation after exposure to 150 mM NaCl, were analysed qualitatively and quantitatively by the NBT assay (Fig. 3). In the Control roots of both Tonkawa and Bianca, a NBT signal was present in the apices of the ARs, and, at a weaker intensity, in the elongation zone and the differentiating vascular system (Fig. 3A arrow, E). In the presence of 150 mM NaCl, both Tonkawa and Bianca ARs showed a signal in the meristematic areas higher than in the Controls (Fig. 3B,F). In Tonkawa ARs, the NBT signal was extended along the forming vascular system (Fig. 3B). In the AR differentiated zone, the signal was very weak in both genotypes whether exposed to salt or not exposed (Fig. 3C-D, G-H). The lateral root primordia (LRP) of both genotypes, not exposed to NaCl, showed the NBT signal in the meristematic apices (Fig. 3C,G). In the presence of salt, there was a reinforced blue colour along the vascular tissues, mainly in the Tonkawa genotype (Fig. 3D). The spectrophotometric analysis of the NBT signal based on the absorbance quantification of the coloured NBT-derivative (formazan), showed that 150 mM NaCl significantly ($p < 0.01$) increase the $O_2^{\bullet-}$ levels in the root system of both genotypes, but particularly in Tonkawa (Fig. 3 I).

3.3. Root meristem is altered by the salt independently on the genotype

The histological analysis was carried out in the apical regions of ARs exposed or not to 150 mM of NaCl to verify if the salt affected root meristem organization and QC definition. In the Control of both genotypes, the AR meristem consisted of small initial cells with dense cytoplasm and large nuclei. These initial cells give rise to extensive root cap, epidermis, cortical parenchyma and to the procambium devoted to producing the vascular cylinder. The AR apex contained a QC, characterized by a small number of quiescent cells (Fig. 4A,E, asterisks), as also known for the PR (Vaughn and Merkle, 1989). In the central region of the AR apex of both genotypes, cells with a precocious distension and differentiation events were present not far from the QC. These cells were the precursors of late metaxylem cells (Fig. 4A,B,E,F, arrows). Cross-sections performed at 300 μm from the tip of the Control ARs showed a regular definition of the radial pattern of the apical meristematic tissues of both genotypes and highlighted the early differentiation phases of the late metaxylem cells differentiation (Fig. 4B, F). The salt treatment led to an altered AR meristem with an irregular QC definition in both Tonkawa and Bianca (Fig. 4C,G, rectangles). Furthermore, a delay and a reduction in the number of the initial cells of the late metaxylem was also evident in the salt-exposed roots (Fig. 4D, H, arrows). Moreover, in the ARs of both genotypes an irregular radial pattern of the meristematic tissues, an early formation of aerenchyma in the cells destined to form the cortical parenchyma (Fig. 4D,H, arrowheads), and an earlier distension of the cells fated to become late metaxylem cells, were also shown (Fig. 4D,H).

3.4. The AR primary structure is salt susceptible, but with differences between the genotypes

The histological analysis carried out on the AR primary structure region of both Bianca and Tonkawa non-exposed to salt showed a similar anatomical organization. This included the epidermis, 6–7 layers of cortical parenchyma, an endodermis characterized by Casparian strip, protoxylem and early metaxylem cells, phloem, late metaxylem and central pith parenchyma cells (Fig. 5A,E). Protoxylem and metaxylem cells were arranged in discrete arches forming a polyarch stele (Fig. 5). Large metaphloem elements associated with companion cells were located between the xylem arches both in the absence and presence of salt (Fig. 5B,F, D, H, and Insets).The late metaxylem cells were delimited by a thin wall without lignification (Fig. 5B,F). To verify if the absence of lignin in the walls of the late metaxylem cells were due to the young age of the roots, the same lignin autofluorescence analysis was carried out on the differentiated region of ARs from plants grown on soil for 1–3 months. The analysis on the ARs of 1-month-old plants revealed lignin deposition on the walls of Bianca late metaxylem cells but not on those of Tonkawa (Supplementary Fig. 2A,B). The same analysis on ARs of 3-months-old plants showed that the walls of the Tonkawa late metaxylem cells were not yet lignified (Supplementary Fig. 2C, D). This result highlighted both a general slow differentiation of these cells, but also a

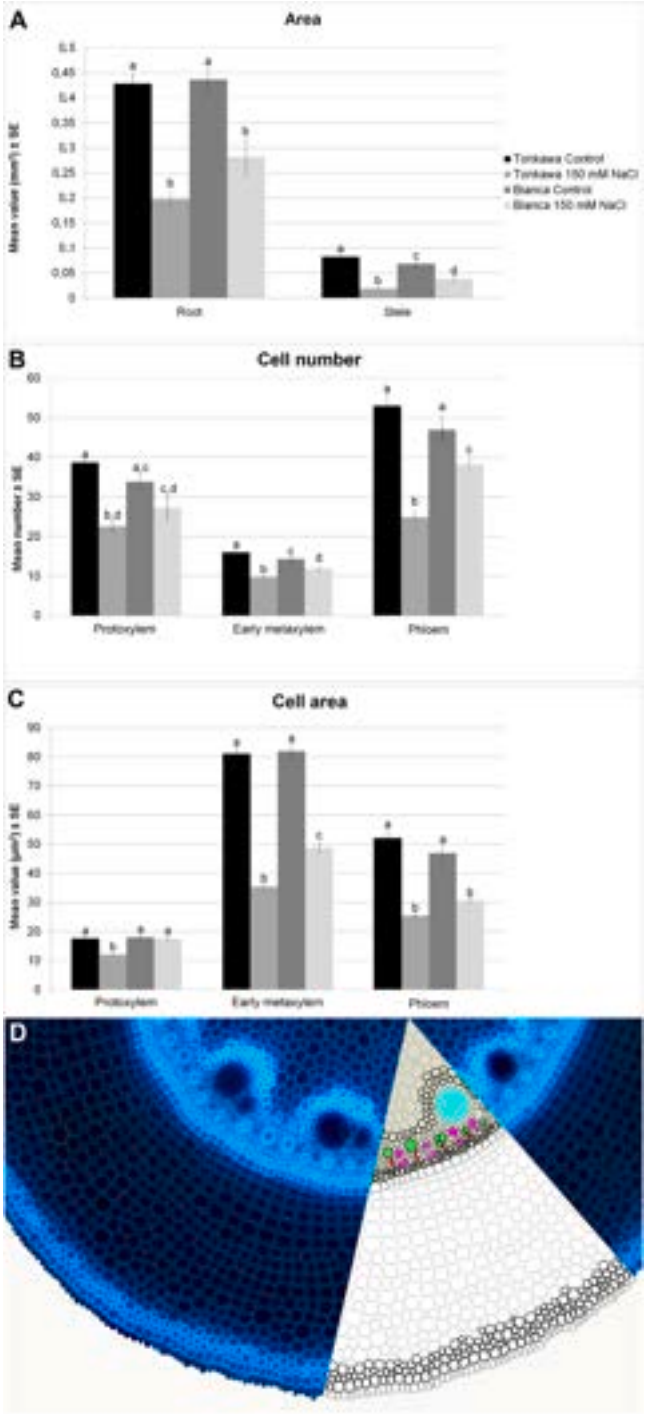

Fig. 6. Mean area (±SE) of root and stele (A), mean number (±SE) of protoxylem, early metaxylem and phloem cells (B) and mean area (±SE) of protoxylem, early metaxylem and phloem cells (C) of Tonkawa and Bianca ARs, at the differentiated region, non-treated (Control) or treated with 150 mM NaCl for 10 days. Data from the three biological replicates. Letters show significant differences for at least $p < 0.05$ between the treatments within the same genotype and organ/tissue. The same letter shows no significant difference within the same genotype and organ/tissue. N = 9 in A and B. N= 60 in C. D, Schematic representation of a sorghum primary root showing measured cells, in red colour protoxylem cells, in dark green early metaxylem cells, in light green late metaxylem cells and in pink phloem cells.

greater ability of Bianca genotype to differentiate such cells in a shorter time than Tonkawa. In both genotypes, the exposure to 150 mM NaCl induced plasmolysis in cortical parenchyma cells (Fig. 5C,G, arrows), and enhanced its transformation into aerenchyma. Moreover, the salt treatment induced an early and accentuated sclerification of the pith parenchyma, starting from its cells bordering the forming late metaxylem cells. However, this effect was more evident in Bianca than in Tonkawa (Fig. 5D,H).

The transverse sections of the Control ARs showed that the mean area of the entire root was similar in both genotypes (Figs. 5A,E and 6A). On the contrary, the mean stele area was significantly ($p < 0.05$) greater in Tonkawa than in Bianca (Fig. 6A). After the salt treatment, the area of the entire root was significantly reduced in comparison with the Control in both genotypes, but the reduction was more consistent in Tonkawa than in Bianca (Figs. 5C,G and 6A). Similarly, the effect of the salt on stele differentiation was also evident. In fact, both Bianca and Tonkawa showed a significant ($p < 0.0001$) reduction of the stele area and again the reduction was more accentuated in Tonkawa than in Bianca (Fig. 6A).

To assess the impact of salt on the vascular system, the protoxylem, metaxylem and phloem elements were counted, and their respective areas measured (Fig. 6B,C,D). In the Control ARs of both genotypes, a similar number of protoxylem cells and a significant ($p < 0.05$) higher number of early metaxylem cells in Tonkawa than in Bianca were observed (Fig. 6B). The salt treatment reduced the AR protoxylem cell number in both genotypes, with a higher reduction ($p < 0.0001$) in Tonkawa (Fig. 6B). Regarding to the early metaxylem elements, their number was reduced by 150 mM NaCl in both genotypes (Fig. 6B). The phloem elements were in similar number in both genotypes and the NaCl treatment significantly reduced it in both, but mainly in Tonkawa (Fig. 6C). The mean area of protoxylem cells was similar in Bianca and Tonkawa Control ARs and the salt significantly ($p < 0.0001$) reduced it in Tonkawa (Fig. 6C). The mean area of the early metaxylem was significantly reduced by salt in both genotypes (Fig. 6C). The phloem showed a similar area in the Control ARs of the two genotypes, with NaCl leading to a significant and similar reduction (Fig. 6C). The salt also affected the formation of the late metaxylem cells. In fact, while Tonkawa and Bianca Control ARs showed a similar mean number of these cells (6.8 ± 0.1 and 6.1 ± 0.5, respectively), the treatment with NaCl reduced their number (4.3 ± 0.3 and 4.9 ± 0.3, respectively) but significantly ($p < 0.001$) in Tonkawa only. The mean area of the late metaxylem in the Control ARs was 2689.34 ± 137 μm^2 in Tonkawa and 2264.15 ± 175 μm^2 in Bianca. The NaCl treatment significantly reduced the late metaxylem mean area in both genotypes (1018 ± 67 μm^2 and 1482 ± 133 μm^2 in Tonkawa and Bianca, respectively).

3.5. Salt stress induces cell wall thickenings in the xylem and endodermis of the ARs with differences between the genotypes

To deepen the analysis on the morpho-functional modifications of sorghum ARs induced by salt, we evaluated and quantified the lignin deposition through lignin autofluorescence detection on the walls of protoxylem, early metaxylem and endodermis cells in the differentiated region of the ARs. In the Control roots, the protoxylem showed a low lignin autofluorescence signal regardless on the genotype (Fig. 7A,C,E). The salt treatment strongly ($p < 0.0001$) enhanced the lignin signal in the protoxylem of Tonkawa ARs and weakly, but significantly ($p < 0.05$) increased it also in Bianca (Fig. 7B,D,E).

The early metaxylem in Tonkawa Control ARs showed a significantly lower lignin signal compared to Bianca (Fig. 7A,C,E). NaCl strongly increased the lignin signal in the Tonkawa early metaxylem but did not change it in Bianca (Fig. 7A,C,E). In the Control ARs, the endodermis cells showed a low lignin signal in Tonkawa and a higher signal in Bianca (Fig. 7A,C,E). The salt treatment induced a strong increase in the lignin deposition in Tonkawa endodermis while it reduced it in Bianca with respect to the Control (Fig. 7B,D,E).

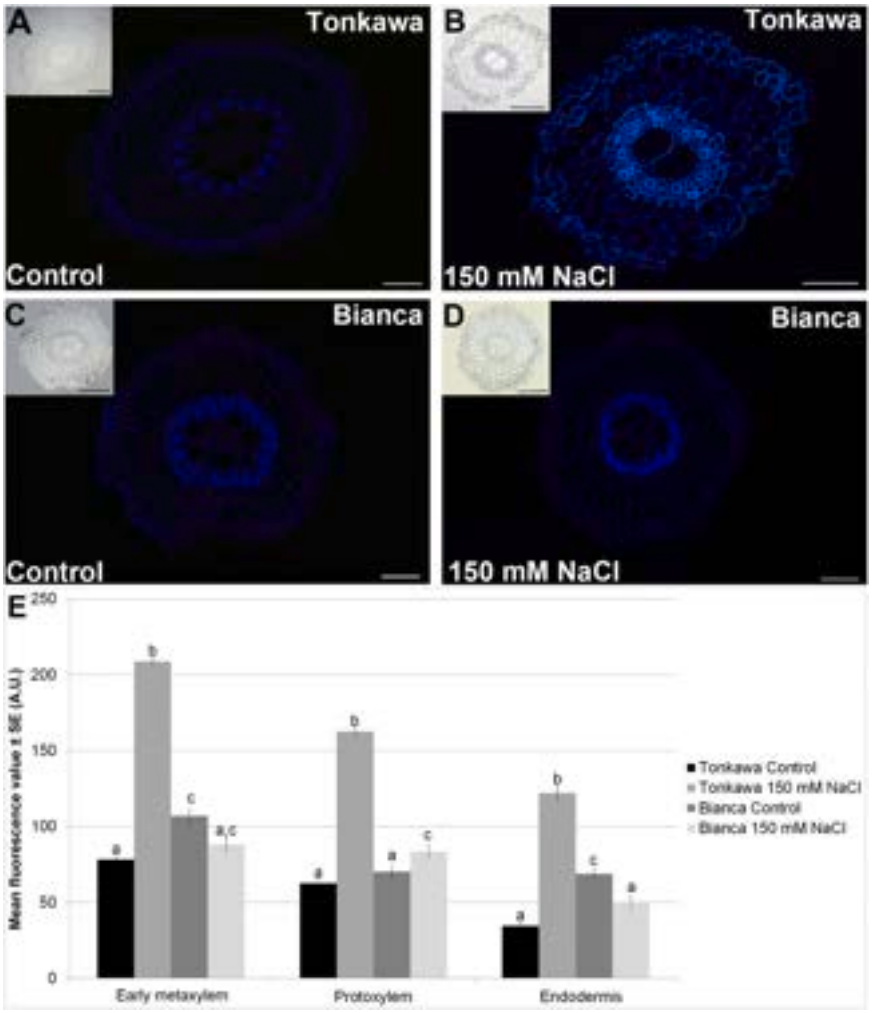

Fig. 7. Transverse sections of Tonkawa and Bianca ARs, at the differentiated region, non-treated (A, C, Control) or treated (B, D) with 150 mM NaCl for 10 days. A-D, images showing lignin autofluorescence (bright blue colour) in protoxylem, early metaxylem and endodermis cell walls. Insets show the same root sections as in A-D under light microscope. Bars = 50 μm. Insets = 100 μm. E, mean values (±SE) of lignin autofluorescence in early metaxylem, protoxylem and endodermis, expressed in Arbitrary Units (AUs). Images and data from the three biological replicates. Different letters show statistical differences, at least at $p < 0.05$ level, between the treatments within the same genotype and the same tissue. The same letter shows no significant difference within the same genotype and tissue. N = 100.

3.6. ^{1}H NMR based metabolomic analysis highlights metabolic differences in salt response between the genotypes

The analysis of the 600 MHz ^{1}H NMR spectra obtained from hydro-alcoholic extracts of roots from Bianca and Tonkawa revealed 33 metabolites including amino acids, organic acids, sugars, organic compounds, secondary metabolites, and other compounds univocally identified. The ^{1}H chemical shifts, multiplicity and the ^{13}C chemical shifts of the identified molecules were reported in Table S1. Examples of ^{1}H NMR spectra are reported in Supplementary Fig. 3 A-E. Quantitative analysis of the chemical composition of Bianca and Tonkawa roots were reported in Table 1. An overview of the whole NMR data set was obtained by applying a preliminary unsupervised PCA performed in Bianca and Tonkawa roots exposed or not to NaCl (Fig. 8A). The first two components explained 74.6 % of the overall variance. A spontaneous grouping to the treatment was identified along the PC1 axis in the PCA score plot (Fig. 8A) and respective loading coefficients were reported in Fig. 8B.

A PCA was carried out also on roots of both genotypes non-exposed to the salt (Supplementary Fig. 4A,B) to highlight the metabolic changes depending on the genotype from those depending on salt treatment. As shown in Supplementary Figure 4B, Bianca genotype showed higher levels of leucine, acetic acid, aspartate, malic acid, allantoin, fumaric acid, tyrosine, phenylalanine, tryptophan and GXP with respect to Tonkawa. Conversely, Tonkawa roots showed higher levels of threonine, alanine, asparagine, glucose, galactose, sucrose, dhurrin, gallic acid, hydroxybenzoate, fumarate and trigonelline compared to Bianca.

To evaluate the metabolic changes occurring in response to salt stress, a PCA analysis was carried out on roots of both genotypes. In Tonkawa roots, 77.6 % of the total variation was explained by the two main components, with PC1 and PC2 contributing 67.7 % and 9.9 %, respectively (Fig. 9). PCA score plot revealed a significant clustering of the samples according to NaCl treatment along the PC1 component (Fig. 9A). The significant variables for the separation of Tonkawa Control and treated roots were reported in Fig. 9B. Tonkawa salt-treated roots showed higher levels of leucine, isoleucine, valine, threonine, alanine, arginine, GABA, asparagine, aspartate, tyrosine, phenylalanine, tryptophan, but also proline, ethanolamine, choline, malic acid, carbohydrates such as glucose, galactose, sucrose, adenosine phosphates nucleotide (AXP), secondary metabolites such as dhurrin and hydroxybenzoate compared to control roots. Guanosine phosphate (GXP) was significantly higher in the Control compared to salt-treated roots, whereas allantoin, uridine phosphate (UXP) and trigonelline did not significantly change.

The PCA carried out on Bianca roots provided a model whose first two components accounted for 82.6 % of the overall variance with PC1

Table 1
^{1}H NMR Chemical composition of hydroalcoholic extracts from Bianca and Tonkawa roots (0.5 mg of root). Means (±SD) denoted by § indicates significant differences compared to Bianca Control; £ indicates significant differences compared to Tonkawa Control; * indicates a $p < 0.05$;** indicates a $p < 0.01$; ç indicates the significance at Kruskal Wallis test compared to Bianca control; &indicates the significance at Kruskal Wallis test compared to Tonkawa Control. AXP: adenosine phosphates nucleotides; GXP: guanosine phosphates nucleotides.

Mean (± SD) mg/100 g	Bianca Control	Bianca NaCl-Treated	Tonkawa Control	Tonkawa NaCl-Treated
	SBRC 1–6	SBRT 1–6	STRC 1–6	STRT 1–6
Leucine	0.858 ± 0.265	7.042 ± 0.866 §**	0.666 ± 0.205	7.024 ± 2.852 £**
Isoleucine	1.124 ± 0.358	5.889 ± 0.998 §**	0.806 ± 0.245	5.503 ± 1.768 £**
Valine	3.77 ± 1.067	11.9 ± 1.953 §**	3.023 ± 0.773	10.443 ± 2.572 £**
Threonine	3.49 ± 0.651	11.155 ± 2.848 §**	3.418 ± 0.863	8.299 ± 2.055 £**
Alanine	5.308 ± 1.191	9.872 ± 1.644 §**	5.976 ± 1.978	9.108 ± 2.182 £*
Arginine	5.471 ± 1.776	22.842 ± 4.269 §**	4.843 ± 1.483	39.515 ± 35.755 &**
Acetic acid	0.091 ± 0.021	0.137 ± 0.065	0.066 ± 0.019	0.118 ± 0.021 &*
Proline	8.465 ± 2.34	59.788 ± 7.094 ç**	6.562 ± 1.656	53.754 ± 18.138 £**
Glutamate	104.902 ± 28.468	229.247 ± 67.911 §**	79.839 ± 23.259	201.028 ± 43.32 £**
Glutamine	10.771 ± 1.572	31.132 ± 3.487 §**	9.629 ± 2.258	28.332 ± 8.18 &**
Aspartate	2.798 ± 1.171	4.854 ± 2.93	2.464 ± 0.472	5.117 ± 1.602 £**
Asparagine	45.397 ± 11.302	61.131 ± 16.787	54.647 ± 10.044	56.171 ± 16.886
GABA	0.891 ± 0.296	1.386 ± 1.325	0.851 ± 0.2	1.205 ± 0.298 £*
Ethanolamine	0.368 ± 0.05	2.826 ± 0.425 ç**	0.371 ± 0.076	2.417 ± 0.583 £**
Choline	1.328 ± 0.158	3.518 ± 0.742 §**	1.31 ± 0.435	2.621 ± 0.472 £**
Malic acid	1.702 ± 0.476	8.216 ± 1.998 §**	1.253 ± 0.366	6.326 ± 1.563 £**
Glucose	235.071 ± 34.318	594.216 ± 137.416 ç**	267.829 ± 68.292	826.009 ± 229.592 £**
Galactose	2.19 ± 0.908	46.482 ± 21.308 ç**	3.884 ± 4.249	58.686 ± 18.516 &**
Allantoin	20.27 ± 4.58	30.789 ± 9.178 §*	19.099 ± 2.967	21.727 ± 12.797
Sucrose	256.387 ± 62.48	921.394 ± 148.724 §**	294.172 ± 113.598	1168.009 ± 217.722 £**
Uridine	0.554 ± 0.132	0.822 ± 0.199 ç*	0.511 ± 0.088	0.619 ± 0.223
UXP	2.101 ± 0.206	2.54 ± 0.23 §**	1.91 ± 0.275	1.91 ± 0.426
Dhurrin	126.648 ± 9.601	162.069 ± 43.874	158.358 ± 21.09	206.882 ± 50.661
AXP	0.968 ± 0.272	3.749 ± 0.646 §**	0.89 ± 0.248	3.214 ± 0.757 £**
Fumaric acid	0.032 ± 0.01	0.073 ± 0.017 §**	0.026 ± 0.005	0.186 ± 0.055 £**
Tyrosine	1.471 ± 0.546	10.374 ± 2.674 ç**	0.732 ± 0.324	10.939 ± 3.905 £**
Gallic acid	0.575 ± 0.061	1.345 ± 0.334 §**	0.937 ± 0.141	1.314 ± 0.51
Phenylalanine	1.798 ± 0.331	13.045 ± 1.712 §**	1.137 ± 0.324	11.298 ± 3.995 £**
Tryptophan	1.365 ± 0.392	5.451 ± 0.988 §**	0.916 ± 0.214	5.507 ± 1.486 £**
Hydroxybenzoate	0.379 ± 0.055	1.578 ± 0.5 §**	0.379 ± 0.099	1.102 ± 0.196 &**
GXP	2.719 ± 1.079	0.427 ± 0.062 §**	1.857 ± 0.824	0.39 ± 0.064 £**
Formic acid	0.118 ± 0.009	0.207 ± 0.085 §*	0.157 ± 0.096	0.246 ± 0.039
Trigonelline	0.118 ± 0.055	0.114 ± 0.022	0.208 ± 0.059	0.199 ± 0.051

and PC2 contributing 74.1 % and 8.5 %, respectively (Fig. 9 C-D). PCA score plot revealed a significant clustering of the samples according to the treatment with NaCl along the PC1 component (Fig. 9C). The significant variables for the separation of samples were reported in Fig. 9D. Differently from Tonkawa, Bianca salt-treated roots showed higher levels of all the identified metabolites compared to Control, except for GXP that was higher in the Control compared to treated roots.

To further highlight the metabolic differences between the genotypes due to salt treatment, a PCA was also carried out on Bianca and Tonkawa-treated roots (Fig. 10) and a core of five metabolites was found. Bianca-treated roots showed higher levels of leucine, isoleucine, alanine, proline and glutamine compared to Tonkawa.

4. Discussion

The performance of the adult plant largely depends on the germination capacity and growth of the seedling, in particular on the early stages of root system development. Only if the root can adapt promptly to the soil conditions, the plant will have the opportunity to grow. For this reason, our research focused on studying the effects of salt stress on the first ten days of seedling growth, and in particular on germination and on the first stages of root system development.

The present results show that both Tonkawa and Bianca genotypes promptly respond to salt stress, activating morpho-anatomical changes in their root system as adaptive mechanisms. Seed germination underwent a significant reduction in the presence of salt in both genotypes, in accordance with what occurs in other sorghum genotypes (Asfaw and Woldemariam, 2008; Zhang et al., 2020). However, Bianca shows a better performance than Tonkawa even in the presence of 300 mM NaCl. This provides a better chance for Bianca to overcome the adverse conditions with a higher salt tolerance. In fact, it is known that salt, depending on the level and genotype, negatively affects germination by creating an osmotic imbalance between culture medium and seed structures/cells, that reduces water uptake by seeds (Jamil et al., 2006; Dehnavi et al., 2020).

We have assessed the morphological changes in PRs and ARs, showing that their length, and consequently their root biomass, were more significantly reduced by the salt in Tonkawa than in Bianca, although Bianca non-exposed to salt had shorter PRs and ARs. It is possible that the reduction in K^{+} and Ca^{2+} ions and sugar availability, induced by NaCl, had a more detrimental effect on the root growth in Tonkawa than Bianca, similarly to what has been reported for other non-tolerant and tolerant sorghum genotypes (Zhang et al., 2020).

Furthermore, we show that other morpho-anatomical changes occur in sorghum ARs, supporting that the adaptation to salinity requires, in addition to rapid osmotic adjustment, structural changes that take longer to implement. These changes alter tissue developmental programs influencing the root system architecture. There are differences between the two genotypes, possibly as an expression of their difference in salt tolerance. In accordance, a modulation of the genome expression has been reported for salt-tolerant sorghum genotypes during extended exposure to non-lethal NaCl concentrations (Fan et al., 2023). Additionally, some genes involved in the early and late stages of root development are upregulated by salt in tolerant sorghum roots (Fan et al.,2023).

Root elongation depends on the regular activity of the apical meristem in all plants. It is known that salt stress induces a decrease in cell expansion, perturbs cell division and root elongation in Arabidopsis and

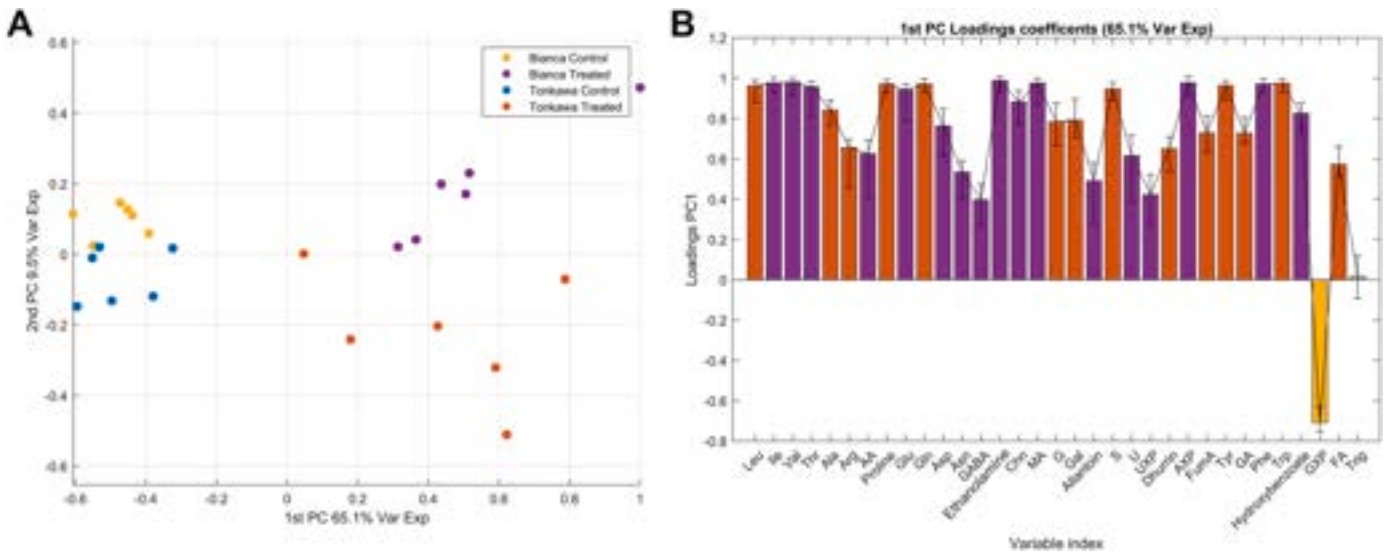

Fig. 8. PCA score plot of Bianca and Tonkawa 10-days-old roots from seedlings treated and untreated with 150 mM NaCl (A). PC1 loading of the treated and untreated roots (B). In purple significant variables higher in Bianca-treated roots, in yellow significant variables higher in Bianca control roots, in orange significant variables higher in Tonkawa-treated roots. Error bars are reported for each loading (0.5 g of roots, see Materials and Methods).

maize (West et al., 2004; Jiang et al., 2017), as well as reduces root meristem size in Arabidopsis (Geng et al., 2013). In accordance, our results show that also in the ARs of Bianca and Tonkawa genotypes the salt similarly alters the organization of the root meristem, mainly by inhibiting the definition of the QC and the surrounding initial cells, thus negatively affecting root elongation. This explains why the ARs of salt-treated seedlings are shorter than the untreated Control in both genotypes, implying that other causes are involved in the greater reduction in length observed in the Tonkawa genotype with respect to Bianca.

One possible explanation could derive from the ROS leves, and in particular, superoxide anion, within the root cells after salt treatment. Indeed, we showed that 150 mM NaCl increased $O2^{\cdot-}$ content in both genotypes but especially in Tonkawa. Thus, it is possible that the highest $O2^{\cdot-}$ in Tonkawa roots, beyond toxicity levels, caused a more pronounced reduction in ARs length with respect to the control than in Bianca.

The most important anatomical parameter discriminating the genotype in response to the salt stress regards the vascular system differentiation, in all its components, i.e. protoxylem, early metaxylem, late metaxylem and phloem. In fact, the salt reduces the mean area of the entire root and its stele more in Tonkawa than in Bianca. The reduction of the entire root area and of the stele are due to both a decrease in the number of protoxylem, early metaxylem, late metaxylem and phloem elements and to their smaller dimensions. In wheat, a high temperature stress causes a decrease in the number of late metaxylem elements in the root apex. This change was considered as an adaptation to limit damage in the root by the changes in water viscosity and hydraulic conductance produced by the stress (Calleja-Cabrera et al., 2020). Also, in sorghum exposed to drought stress a reduction of hydraulic conductance is observed in the roots, and this was correlated with the persistence of immature late xylem elements and smaller diameter and lower number of protoxylem and early maturing metaxylem (Cruz et al., 1992). It has been suggested that the stress-responsive decreases in metaxylem area in different sorghum genotypes are advantageous under drought, particularly when balancing water uptake with transpiration water loss (Lovisolo and Schubert, 1998; Guha et al., 2018; Priatama et al., 2022; Lehrer and Hawkins, 2023). Moreover, the sorghum drought-sensitive genotypes would undergo a stronger modification in xylem traits (e.g. vessel size, number and distribution) along with a stronger reduction in plant size and leaf area reduction than less drought-sensitive genotypes (Lehrer and Hawkins, 2023). In accordance, the present data show that the metaxylem and protoxylem cells were reduced in number and dimension with major effects in the more salt-sensitive (i.e. Tonkawa) genotype compared to the tolerant genotype (i.e. Bianca). The phloem is also altered by salt stress. In sorghum it has been demonstrated that in the leaves, xylem and phloem anatomy under water stress are finely correlated (Guha et al., 2018). Our data show that, in sorghum roots, salt induces similar modifications in xylem and phloem, sustaining that also in the root all the components of vascular system are finely connected. As here reported, phloem differentiation, mainly as element number, is less reduced in Bianca than Tonkawa, suggesting that more phloem elements are needed in the root of the tolerant genotype. In accordance, it was reported that the salt tolerant sorghum transfers more sucrose to the root as compared to the susceptible one, with this involving more phloem elements (Abuslima et al., 2022). It is also possible that greater amounts of solutes help the root to restore the osmotic imbalance between the growth medium and the inside of the cells. Altogether, the less reduction of all the components of the root vasculature under salt stress indicates a more effective stress tolerance response in Bianca compared to Tonkawa. The present data also show that salt induces a strong lignification in protoxylem, metaxylem and endodermis cell walls of Tonkawa ARs. On the contrary, in Bianca, the same cells exhibited walls with a lignin deposition lower or like those of cells not exposed to salt. These findings highlight that the genotype showing lower tolerance to salt activates the lignification with a dual function, to limit the entry of an excess of Na^+ ions into the cells, and to prevent water radial apoplastic flow to maintain cellular turgor. Similar results were reported for grapevine and another sorghum genotype exposed to water stress (Cruz et al., 1992; Choat et al., 2010). We observed a reduced lignification in the metaxylem and endodermis cell walls after salt exposure in Bianca ARs. It is interesting to note that, when Bianca was not exposed to salt, the lignification of the cell walls of the metaxylem and endodermis was always higher than in untreated Tonkawa ARs. It is possible that the increased lignin synthesis observed in Tonkawa under salt-stress, beyond what is necessary to counteract the toxicity of the non-lethal salt level, has taken away energy and metabolites necessary for other metabolic processes thus contributing to reduce the fitness of this genotype resulting into salt sensitivity.

We show that also the reduction of the lumen of the metaxylem and protoxylem is associated with an increase of lignin deposition in the cell wall, mainly in the sensitive genotype, probably to withstand the

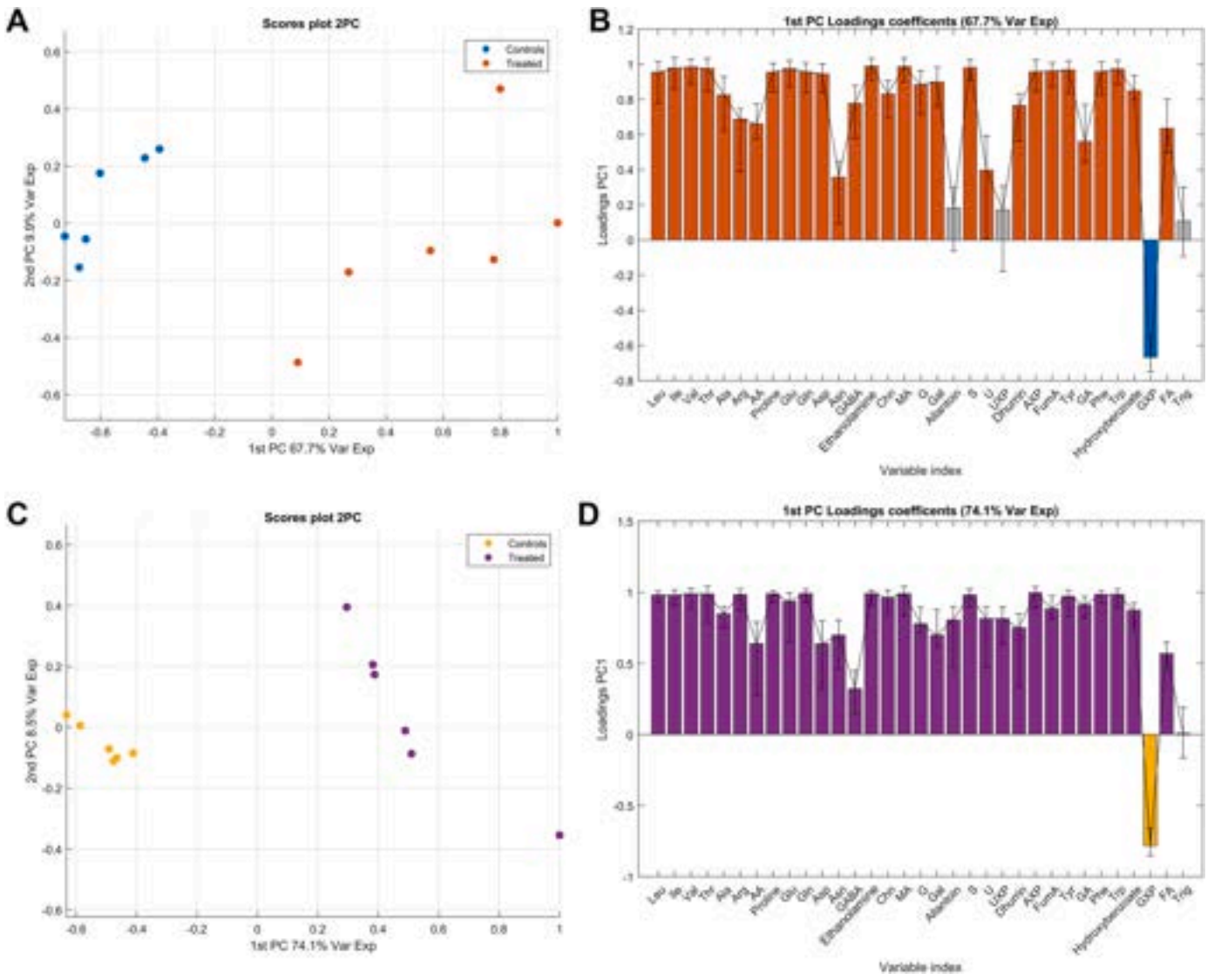

Fig. 9. PCA score plot of Tonkawa untreated (Control) and NaCl treated roots (A). PC1 loading coefficients of the treated roots (B). In orange significant variables higher in treated compared to Control roots, in blue significant variables higher in Control compared to treated roots, in grey unchanged variables. PCA score plot of Bianca untreated (Control) and NaCl treated roots (C). PC1 loading coefficients of the treated roots (D). In purple significant variables higher in treated compared to Control roots, in yellow significant variables higher in control compared to treated roots. Error bars are reported for each loading (0.5 g of roots, see Materials and Methods).

pressure in the xylem due to the salt, as reported for other sorghum genotypes (Karumanchi et al., 2023). Altogether, the present data provide evidence that salt induces genotype- dependent changes, either increasing or decreasing the lignin deposition on the cell walls of tissues that act as a barrier or that are involved in transport.

The metabolomic analysis of sorghum roots exposed to salt revealed common metabolic threads in Bianca and Tonkawa involving significant changes in nucleotides, GS/GOGAT cycle, amino acid and carbohydrate metabolism, proline synthesis, TCA cycle, organic acids and secondary metabolites. Most of the assigned metabolites significantly increased in salt-treated roots compared to Controls, except for GXP (ATP/ADP/AMP) that decreased in both genotypes. According to the metabolomic profile, Bianca and Tonkawa roots exposed to salt altered the metabolic activity to maintain turgor pressure that is affected by excessive amounts of ions. In this context, both genotypes presented a high osmoregulatory capacity exhibiting a significant increase in their osmolytes, but with some differences depending on the genotype.

We show that allantoin and trigonelline levels were increased by salt in the roots of Bianca but not of Tonkawa. Allantoin has been reported to be involved in plant salt tolerance (Kaur et al., 2021). In fact, its levels increase under salt stress in different plant species and organs, such as rye roots (Sagi et al., 1997), *Crithmum maritimum* leaves (Ventura et al., 2014) and roots of salt-susceptible and, mainly, salt-tolerant rice genotypes (Wang et al., 2016). Similarly, trigonelline has been also proposed to prevent water loss in response to a salt excess (Minorsky, 2002). Thus, it is possible that the greater accumulation of these metabolites in Bianca, after salt exposure, contributes to the greater salt tolerance of this genotype compared to Tonkawa. Furthermore, both genotypes accumulate more proline after NaCl treatment. Proline accumulation occurs naturally under salinity stress, because also this amino acid acts as osmo-protectant. A high level of proline, due to either new synthesis or inhibition of oxidation in the mitochondria, reduces the cell water potential below the external water potential, enhancing the water flow into the cells to maintain cellular water status and plant cell turgidity (Huang et al., 2013; Meena et al., 2019; El Moukhtari et al., 2020; Nguyen et al., 2021). However, present data also show differences in proline levels between the two genotypes, with Bianca exhibiting higher levels than Tonkawa, suggesting that higher levels of this

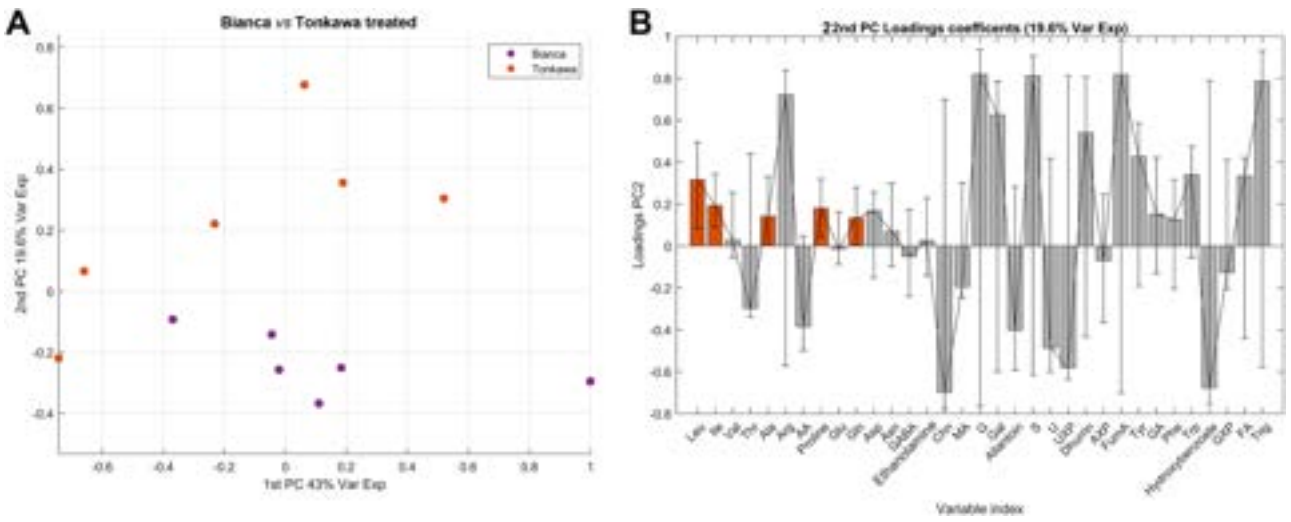

Fig. 10. PCA score plot of Bianca *vs* Tonkawa salt-treated roots (A). PC2 loading coefficients of the treated roots (B). In orange significant variables higher in Bianca compared to Tonkawa - treated roots, in grey non-significant variables. Error bars are reported for each loading (0.5 g of roots, see Materials and Methods).

osmo-protectant facilitate its better salt tolerance.

Moreover, Bianca salt-treated roots showed significantly higher leucine, isoleucine, alanine, and glutamate levels compared to those of Tonkawa. Considering that the increase of Na^+ and Cl^-ions requires the accumulation of solutes in the cell, the increase of these osmo-regulators could enhance plant stress tolerance by playing a role in both osmo-protection through ROS homeostasis and redox regulation, as well as in ionic balance and osmotic adjustment (Xiao and Zhou, 2023).

The salt is known to enhance energy consumption and ROS production (Bandehagh and Taylor, 2020), for this reason the modulation of energy metabolism is essential for a response to salinity. Mitochondrial respiration during salt exposure is needed to produce more ATP, which provides energy for ion exclusion, synthesis of compatible solutes and detoxification of ROS (Munns and Tester, 2008). The observed increases in AXP levels in both genotypes and, mainly, of UXP only in Bianca-treated roots are consistent with the higher requirement of ATP and UDP under salt, and highlight a better response for Bianca.

Interestingly, our results showed that the salt treatment strongly increased lignin deposition in Tonkawa, but reduced it in Bianca, particularly in the cell walls of metaxylem and endodermis, which are tissues destined to function longer than the protoxylem. Lignin biosynthesis involves the biosynthesis of lignin monomers deriving from phenylpropanoid metabolism whose precursors are tyrosine, phenylalanine and tryptophan (Liu et al., 2018). Interestingly, Bianca Control roots showed higher levels of these aromatic amino acids compared to Tonkawa suggesting less need for Bianca to supply precursors to synthetize lignin under salt stress, as also confirmed by anatomical results.

5. Conclusions

The present results contributed to a deeper understanding of the anatomical changes of the root system in response to salt stress in an important crop such as sorghum. Changes in vascular tissues differentiation, cell wall lignification in metaxylem and endodermis of ARs, as well as changes in root metabolome are proposed as selective markers of genotype salt susceptibility or tolerance. They also highlight the possibility for the cultivation of Bianca genotype to recover marginal areas characterized by salt stress, as well as its suitability for use as germplasm material in sorghum breeding programs.

Funding

The work was supported by the European Union Next-Generation EU (PIANO NAZIONALE DI RIPRESA E RESILIENZA (PNRR)—MISSIONE 4 COMPONENTE 2, INVESTIMENTO 1.4—D.D. 103217/06/2022, CN00000022, Agritech National Research Center) to G.F. and E.B.

CRediT authorship contribution statement

Diego Piacentini: Methodology, Formal analysis, Data curation. **Alice Peduzzi:** Methodology, Data curation, Conceptualization. **Federica Della Rovere:** Methodology, Formal analysis, Data curation. **Elisa Brasili:** Methodology, Investigation, Funding acquisition. **Simone D′ Angeli:** Methodology. **Adriano Patriarca:** Methodology. **Maria Maddalena Altamura:** Writing – review & editing, Writing – original draft. **Giuseppina Falasca:** Writing – review & editing, Writing – original draft, Validation, Supervision, Funding acquisition, Data curation, Conceptualization.

Declaration of Competing Interest

The authors declare that they have no known competing financial interests or personal relationships that could have appeared to influence the work reporter in this paper.

Acknowledgments

We are grateful to Padana Sementi Elette S.r.l for providing the seeds of Bianca and Tonkawa genotypes.

Author agreement statement

The co-authors, Peduzzi, A, Piacentini A., Brasili E., Della Rovere F., Patriarca A., D'Angeli S., Altamura M.M. and Falasca G. declare that this manuscript is original, has not been published before and is not currently being considered for publication elsewhere.

They confirm that the manuscript has been read and approved by all named authors and that there are no other persons who satisfied the criteria for authorship but are not listed.

They further confirm that the order of authors listed in the manuscript has been approved by all of us.

They understand that the Corresponding Author, Falasca G., is the sole contact for the Editorial process.

She is responsible for communicating with the other authors about progress, submissions of revisions and final approval of proofs

Author contributions

Peduzzi Alice: conceptualization, methodology and elaboration data; Piacentini Diego and Della Rovere Federica: Histological methodology and formal analysis; Brasili Elisa, Patriarca Adriano: metabolomic methodology and data mining; D'Angeli Simone: fluorescence methodology; Altamura Maria Maddalena: review and editing the draft; Falasca Giuseppina: conceptualization, elaboration data, writing, review and editing the draft.

Appendix A. Supporting information

Supplementary data associated with this article can be found in the online version at doi:10.1016/j.envexpbot.2024.105876.

References

Abuslima, E., Kanbar, A., Raorane, M.L., Eiche, E., Junker, B.H., Hause, B., Riemann, M., Nick, P., 2022. Gain time to adapt: how sorghum acquires tolerance to salinity. Front. Plant Sci. 13, 1008172 https://doi.org/10.3389/fpls.2022.1008172.

Acosta-Motos, J.R., Ortuño, M.F., Bernal-Vicente, A., Diaz-Vivancos, P., Sanchez-Blanco, M.J., Hernandez, J.A., 2017. Plant responses to salt stress: adaptive mechanisms. Agronomy 7, 18. https://doi.org/10.3390/agronomy7010018.

Agati, G., Biricolti, S., Guidi, L., Ferrini, F., Fini, A., Tattini, M., 2011. The biosynthesis of flavonoids is enhanced similarly by UV radiation and root zone salinity in *L. vulgare* leaves. J. Plant Physiol. 168, 204–2012. https://doi.org/10.1016/j.jplph.2010.07.016.

Asfaw, K.G., Woldemariam, M.G., 2008. Response of some lowland growing sorghum (*Sorghum bicolor* L. Moench) accessions to salt stress during germination and seedling growth. Afr. J. Agric. Res. 3, 44–48.

Babamoradi, H., van den Berg, F., Rinnan, Å., 2013. Bootstrap based confidence limits in principal component analysis—A case study. Chemom. Intell. Lab. 120, 97–105. https://doi.org/10.1016/j.chemolab.2012.10.007.

Balasubramaniam, T., Shen, G., Esmaeili, N., Zhang, H., 2023. Plants' response mechanisms to salinity stress. Plants 12, 2253. https://doi.org/10.3390/plants12122253.

Bandehagh, A., Taylor, N.L., 2020. Can alternative metabolic pathways and shunts overcome salinity induced inhibition of central carbon metabolism in crops? Front. Plant Sci. 11, 1072. https://doi.org/10.3389/fpls.2020.01072.

Brown, M.B., Forsythe, A.B., 1974. Robust tests for equality of variances. J. Am. Stat. Assoc. 69, 364–367. https://doi.org/10.2307/2285659.

Calleja-Cabrera, J., Boter, M., Oñate-Sánchez, L., Pernas, M., 2020. Root growth adaptation to climate change in crops. Front. Plant Sci. 11, 544. https://doi.org/10.3389/fpls.2020.00544.

Calone, R., Sanoubar, R., Lambertini, C., Speranza, M., Vittori Antisari, L., Vianello, G., Barbanti, L., 2020. Salt tolerance and Na allocation in *Sorghum bicolor* under variable soil and water salinity. Plants 9, 561. https://doi.org/10.3390/plants9050561.

Chan, C., Lam, H.M., 2014. A putative lambda class glutathione S-transferase enhances plant survival under salinity stress. Plant Cell Physiol. 55, 570–579. https://doi.org/10.1093/pcp/pct201.

Chandran, A.K.N., Kim, J.W., Yoo, Y.H., Park, H.L., Kim, Y.J., Cho, M.H., Jung, K.H., 2019. Transcriptome analysis of rice-seedling roots under soil–salt stress using RNA-Seq method. Plant Biotechnol. Rep. 13, 567–578. https://doi.org/10.1007/s11816-019-00550-3.

Choat, B., Drayton, W.M., Brodersen, C., Matthews, M.A., Shackel, K.A., Wada, H., McElrone, A.J., 2010. Measurement of vulnerability to water stress-induced cavitation in grapevine: a comparison of four techniques applied to a long-vesseled species. Plant Cell Environ. 33, 1502–1512. https://doi.org/10.1111/j.1365-3040.2010.02160.x.

Cruz, R.T., Jordan, W.R., Drew, M.C., 1992. Structural changes and associated reduction of hydraulic conductance in roots of *Sorghum bicolor* L. following exposure to water deficit. Plant Physiol. 99, 203–212. https://doi.org/10.1104/pp.99.1.203.

Currier, H.B., Strugger, S., 1956. Aniline blue and fluorescence microscopy of callose in bulb scales of *Allium cepa* L. Protoplasma 45, 552–559. https://doi.org/10.1007/BF01252676.

Dehnavi, A.R., Zahedi, M., Ludwiczak, A., Cardenas Perez, S., Piernik, A., 2020. Effect of salinity on seed germination and seedling development of sorghum (*Sorghum bicolor* (L.) Moench) genotypes. Agronomy 10, 859. https://doi.org/10.3390/agronomy10060859.

Demecsová, L., Zelinová, V., Liptáková, L., Valentovičová, K., Tamás, L., 2020. Indole-3-butyric acid priming reduced cadmium toxicity in barley root tip via NO generation and enhanced glutathione peroxidase activity. Planta 252, 1–16. https://doi.org/10.1007/s00425-020-03451-w.

El Moukhtari, A., Cabassa-Hourton, C., Farissi, M., Savouré, A., 2020. How does proline treatment promote salt stress tolerance during crop plant development? Front. Plant Sci. 11, 1127. https://doi.org/10.3389/fpls.2020.01127.

El Omari, R., Nhiri, M., 2015. Adaptive response to salt stress in sorghum (*Sorghum bicolor*). Am. Eurasia J. Agric. Environ. Sci. 15, 1351–1360. https://doi.org/10.5829/idosi.aejaes.2015.15.7.12683.

Eriksson, L., Byrne, T., Johansson, E., Trygg, J., Vikström, C., 2013. Multi- and megavariate data analysis basic principles and applications. 3rd edition. Malmö (Sweden): MKS UmetricsAB.

Fan, S., Chen, J., Yang, R., 2023. Candidate genes for salt tolerance in forage sorghum under saline conditions from germination to harvest maturity. Genes-Basel 14, 293. https://doi.org/10.3390/genes14020293.

Foronda, D.A., 2022. Reclamation of a saline-sodic soil with organic amendments and leaching. Environ. Sci. Proc. 16, 56. https://doi.org/10.3390/environsciproc2022016056.

Geng, Y., Wu, R., Wee, C.W., Xie, F., Wei, X., Chan, P.M., Tham, C., Duan, L., Dinneny, J. R., 2013. A spatio-temporal understanding of growth regulation during the salt stress response in Arabidopsis. Plant Cell 25, 2132–2154. https://doi.org/10.1105/tpc.113.112896.

Giampaoli, O., Sciubba, F., Conta, G., Capuani, G., Tomassini, A., Giorgi, G., Brasili, E., Aureli, W., Miccheli, A., 2021. Red beetroot's NMR-based metabolomics: phytochemical profile related to development time and production year. Foods 10, 1887. https://doi.org/10.3390/foods10081887.

Guha, A., Chhajed, S.S., Choudhary, S., Sunny, R., Jansen, S., Barua, D., 2018. Hydraulic anatomy affects genotypic variation in plant water use and shows differential organ specific plasticity to drought in Sorghum bicolor. Environ. Exp. Bot. 156, 25–37. https://doi.org/10.1016/j.envexpbot.2018.08.025.

Gupta, B., Huang, B., 2014. Mechanism of salinity tolerance in plants: physiological, biochemical, and molecular characterization. Int. J. Genom. 2014, 701596 https://doi.org/10.1155/2014/701596.

Henderson, A.N., Crim, P.M., Cumming, J.R., Hawkins, J.S., 2020. Phenotypic and physiological responses to salt exposure in sorghum reveal diversity among domesticated landraces. Am. J. Bot. 107, 983–992. https://doi.org/10.1002/ajb2.1506.

Huang, R., 2018. Research progress on plant tolerance to soil salinity and alkalinity in sorghum. J. Integr. Agr. 17, 739–746. https://doi.org/10.1016/S2095-3119(17)61728-3.

Huang, Z., Zhao, L., Chen, D., Liang, M., Liu, Z., Shao, H., Long, X., 2013. Salt stress encourages proline accumulation by regulating proline biosynthesis and degradation in *Jerusalem artichoke* plantlets. PLoS ONE 8, e62085. https://doi.org/10.1371/journal.pone.0062085.

Impa, S.M., Perumal, R., Bean, S.R., Sunoj, V.S.J., Jagadish, S.V.K., 2019. Water deficit and heat stress induced alterations in grain physico-chemical characteristics and micronutrient composition in field grown grain sorghum. J. Cereal Sci. 86, 124–131. https://doi.org/10.1016/j.jcs.2019.01.013.

Jamil, M., Deog Bae, L., Kwang Yong, J., Ashraf, M., Sheong Chun, L., Eui Shik, R., 2006. Effect of salt (NaCl) stress on germination and early seedling growth of four vegetables species. J. Cent. Eur. Agric. 7, 273–282.

Jiang, C., Zu, C., Lu, D., Zheng, Q., Shen, J., Wang, H., Li, D., 2017. Effect of exogenous selenium supply on photosynthesis, Na^+ accumulation and antioxidative capacity of maize (*Zea mays* L.) under salinity stress. Sci. Rep. 7, 42039 https://doi.org/10.1038/srep42039.

Karumanchi, A.R., Sivan, P., Kummari, D., Rajasheker, G., Kumar, S.A., Reddy, P.S., Suravajhala, P., Podha, S., Kishor, P.B.K., 2023. Root and leaf anatomy, ion accumulation, and transcriptome pattern under salt stress conditions in contrasting genotypes of *Sorghum bicolor*. Plants 12, 2400. https://doi.org/10.3390/plants12132400.

Kaur, H., Chowrasia, S., Gaur, V.S., Mondal, T.K., 2021. Allantoin: emerging role in plant abiotic stress tolerance. Plant Mol. Biol. Rep. 39, 648–661. https://doi.org/10.1007/s11105-021-01280-z.

Krishnamurthy, L., Serraj, R., Hash, C.T., Dakheel, A.J., Reddy, B.V.S., 2007. Screening sorghum genotypes for salinity-tolerant biomass production. Euphytica 156, 15–24. https://doi.org/10.1007/s10681-006-9343-9.

Lehrer, M.A., Hawkins, J.S., 2023. Plant height shapes hydraulic architecture but does not predict metaxylem area under drought in *Sorghum bicolor*. Plant Direct 7, e498. https://doi.org/10.1002/pld3.498.

Liu, Q., Luo, L., Zheng, L., 2018. Lignins: biosynthesis and biological functions in plants. Int. J. Mol. Sci. 19, 335. https://doi.org/10.3390/ijms19020335.

Lovisolo, C., Schubert, A., 1998. Effects of water stress on vessel size and xylem hydraulic conductivity in Vitis vinifera L. J. Exp. Bot. 49, 693–700. https://doi.org/10.1093/jxb/49.321.693.

Mansour, M.M., 2014. The plasma membrane transport systems and adaptation to salinity. J. Plant Physiol. 171, 1787–1800. https://doi.org/10.1016/j.jplph.2014.08.016.

Mansour, M.M.F., Emam, M.M., Salama, K.H.A., Morsy, A.A., 2021. Sorghum under saline conditions: responses, tolerance mechanisms, and management strategies. Planta 254, 24. https://doi.org/10.1007/s00425-021-03671-8.

Mansour, M.M.F., Salama, K.H.A., Morsy, A.A., Emam, M.M., 2020. Plasma membrane lipids and adaptation of plants to salt stress. In: Daniel JA, ed. Advances in Environmental Research vol. 78, 1–111. ISBN: 978-1-53618-774-8.

Mbinda, W., Kimtai, M., 2019. Evaluation of morphological and biochemical characteristics of sorghum [*Sorghum bicolor* [L.] Moench] varieties in response salinity stress. Annu. Res. Rev. Biol. 33, 1–9. https://doi.org/10.9734/arrb/2019/v33i130110.

Meena, M., Divyanshu, K., Kumar, S., Swapnil, P., Zehra, A., Shukla, V., Yadav, M., Upadhyay, R.S., 2019. Regulation of L-proline biosynthesis, signal transduction, transport, accumulation and its vital role in plants during variable environmental conditions. Heliyon 5, e02952. https://doi.org/10.1016/j.heliyon.2019.e02952.

Minorsky, P.V., 2002. The hot and the classic. Plant Physiol. 128, 7–8.

Mohanavel, W., Boopathi, N.M., Muthurajan, R., Senthil, A., 2020. *In vitro* root architectural screening for early drought adaptive traits in sorghum (*Sorghum bicolor*

L.). Int. J. Curr. Microbiol. Appl. Sci. 9, 3161–3167. https://doi.org/10.20546/ijcmas.2020.905.375.
Moreno-Villena, J.J., Zhou, H., Gilman, I.S., Tausta, S.L., Cheung, C.Y.M., Edwards, E.J., 2022. Spatial resolution of an integrated C_4+CAM photosynthetic metabolism. Sci. Adv. 8, eabn2349 https://doi.org/10.1126/sciadv.abn2349.
Munns, R., Tester, M., 2008. Mechanisms of salinity tolerance. Annu. Rev. Plant Biol. 59, 651–681. https://doi.org/10.1146/annurev.arplant.59.032607.092911.
Murashige, T., Skoog, F., 1962. A revised medium for rapid growth and bio assays with tobacco tissue cultures. Physiol. Plant. 15, 473–497. https://doi.org/10.1111/j.1399-3054.1962.tb08052.x.
Nguyen, H.T.T., Das Bhowmik, S., Long, H., Cheng, Y., Mundree, S., Hoang, L.T.M., 2021. Rapid accumulation of proline enhances salinity tolerance in Australian wild rice *Oryza australiensis* Domin. Plants 10, 2044. https://doi.org/10.3390/plants10102044.
de Oliveira, D.F., de, Sousa, Lopes, L., Gomes-Filho, E., 2020. Metabolic changes associated with differential salt tolerance in sorghum genotypes. Planta 252, 34. https://doi.org/10.1007/s00425-020-03437-8.
Pantha, P., Dassanayake, M., 2020. Living with salt. Innovation 1, 100050. https://doi.org/10.1016/j.xinn.2020.100050.
Peluso, A., Glen, R., Ebbels, T.M.D., 2021. Multiple-testing correction in metabolome-wide association studies. BMC Bioinforma. 22, 67. https://doi.org/10.1186/s12859-021-03975-2.
Piacentini, D., Ronzan, M., Fattorini, L., Della Rovere, F., Massimi, L., Altamura, M.M., Falasca, G., 2020. Nitric oxide alleviates cadmium- but not arsenic-induced damages in rice roots. Plant Physiol. Bioch. 151, 729–742. https://doi.org/10.1016/j.plaphy.2020.04.004.
Pound, M.P., French, A.P., Atkinson, J.A., Wells, D.M., Bennett, M.J., Pridmore, T., 2013. RootNav: navigating images of complex root architectures. Plant Physiol. 162, 1802–1814. https://doi.org/10.1104/pp.113.221531.
Priatama, R.A., Heo, J., Kim, S.H., et al., 2022. Narrow lpa1 metaxylems enhance drought tolerance and optimize water use for grain filling in dwarf rice. Front. Plant Sci. 13, 894545 https://doi.org/10.3389/fpls.2022.894545.
Ren, G., Yang, P., Cui, J., Gao, Y., Yin, C., Bai, Y., Zhao, D., Chang, J., 2022. Multiomics analyses of two sorghum cultivars reveal the molecular mechanism of salt tolerance. Front. Plant Sci. 13, 886805 https://doi.org/10.3389/fpls.2022.886805.
Ronzan, M., Piacentini, D., Fattorini, L., Della Rovere, F., Eiche, F., Riemann, E., Altamura, M.M., Falasca, G., 2018. Cadmium and arsenic affect root development in *Oryza sativa* L. negatively interacting with auxin. Environ. Exp. Bot. 151, 64–75. https://doi.org/10.1016/j.envexpbot.2018.04.008.
Sagi, M., Savidov, N.A., L'vov, N.P., Lips, S.H., 1997. Nitrate reductase and molybdenum cofactor in annual ryegrass as affected by salinity and nitrogen source. Physiol. Plant. 99, 546–553. https://doi.org/10.1111/j.1399-3054.1997.tb05355.x.
Shi, X., Zhou, Y., Zhao, X., Guo, P., Ren, J., Zhang, H., Dong, Q., Zhang, Z., Yu, H., Wan, S., 2023. Soil metagenome and metabolome of peanut intercropped with sorghum reveal a prominent role of carbohydrate metabolism in salt-stress response. Environ. Exp. Bot. 209, 105274 https://doi.org/10.1016/j.envexpbot.2023.105274.
Spinelli, V., Brasili, E., Sciubba, F., Ceci, A., Giampaoli, O., Miccheli, A., Pasqua, G., Persiani, A.M., 2022. Biostimulant effects of *Chaetomium globosum* and *Minimedusa polyspora* culture filtrates on *Cichorium intybus* plant: growth performance and metabolomic traits. Front. Plant Sci. 13, 879076 https://doi.org/10.3389/fpls.2022.879076.
Stevens, J.,P., 2007. Intermediate Statistics: A Modern Approach, third edition. Routledge, New York.
Vaughn, S.F., Merkle, M.G., 1989. Histological and cytological effects of haloxyfop on sorghum (*Sorghum bicolor*) and unicorn-plant (*Proboscidea louisianica*) root meristems. Histological and cytological effects of haloxyfop on sorghum (*Sorghum bicolor*) and unicorn-plant (*Proboscidea louisianica*) root meristems. Weed Sci. 37, 503–511.
Ventura, Y., Myrzabayeva, M., Alikulov, Z., Omarov, R., Khozin-Goldberg, I., Sagi, M., 2014. Effects of salinity on flowering, morphology, biomass accumulation and leaf metabolites in an edible halophyte. AoB Plants 6, plu053. https://doi.org/10.1093/aobpla/plu053.
Wang, W.S., Zhao, X.Q., Li, M., Huang, L.Y., Xu, J.L., Zhang, F., Cui, Y.R., Fu, B.Y., Li, Z. K., 2016. Complex molecular mechanisms underlying seedling salt tolerance in rice revealed by comparative transcriptome and metabolomic profiling. J. Exp. Bot. 67, 405–419. https://doi.org/10.1093/jxb/erv476.
West, G., Inzé, D., Beemster, G.T.S., 2004. Cell cycle modulation in the response of the primary root of Arabidopsis to salt stress. Plant Physiol. 135, 1050–1058. https://doi.org/10.1104/pp.104.040022.
Xiao, F., Zhou, H., 2023. Plant salt response: perception, signaling, and tolerance. Front. Plant Sci. 13, 1053699 https://doi.org/10.3389/fpls.2022.1053699.
Yan, J., Wang, B., Jiang, Y., Cheng, L., Wu, T., 2014. GmFNSII-controlled soybean flavone metabolism responds to abiotic stresses and regulates plant salt tolerance. Plant Cell Physiol. 55, 74–86. https://doi.org/10.1093/pcp/pct159.
Zhang, F., Sapkota, S., Neupane, A., Yu, J., Wang, Y., Zhu, K., Lu, F., Huang, R., Zou, J., 2020. Effect of salt stress on growth and physiological parameters of sorghum genotypes at an early growth stage. Indian J. Exp. Biol. 58, 404–411.
Zhang, H., Wang, R., Wang, H., et al., 2019. Heterogeneous rootzone salinity mitigates salt injury to *Sorghum bicolor* (L.) Moench in a split-root system. PLoS ONE 14, e0227020. https://doi.org/10.1371/journal.pone.0227020.